ornl

OAK RIDGE NATIONAL LABORATORY

UNION CARBIDE

OPERATED BY
UNION CARBIDE CORPORATION
FOR THE UNITED STATES
DEPARTMENT OF ENERGY

NUREG/CR-3335
ORNL/TM-8793

Data Summary Report for Fission Product Release Test HI-3

M. F. Osborne
R. A. Lorenz
K. S. Norwood
J. R. Travis
C. S. Webster

Prepared for the
U.S. Nuclear Regulatory Commission
Office of Nuclear Regulatory Research
Under Interagency Agreement DOE 40-551-75

Printed in the United States of America. Available from
National Technical Information Service
U.S. Department of Commerce
5285 Port Royal Road, Springfield, Virginia 22161

Available from

GPO Sales Program
Division of Technical Information and Document Control
U.S. Nuclear Regulatory Commission
Washington, D.C. 20555

NUREG/CR-3335
ORNL/TM-8793
Dist. Category R3

Chemical Technology Division

DATA SUMMARY REPORT FOR FISSION PRODUCT RELEASE TEST HI-3

M. F. Osborne
R. A. Lorenz
K. S. Norwood*
J. R. Travis
C. S. Webster

*Guest scientist from UKAEA.

Manuscript Completed — August 1983
Date of Issue — March 1984

Prepared for the
U.S. Nuclear Regulatory Commission
Office of Nuclear Regulatory Research
Washington, DC 20555
under Interagency Agreement DOE 40-551-75

NRC FIN No. B0127

Prepared by the
OAK RIDGE NATIONAL LABORATORY
Oak Ridge, Tennessee 37831
operated by
UNION CARBIDE CORPORATION
for the
U.S. DEPARTMENT OF ENERGY
under Contract No. W-7402-eng-26

ABSTRACT

The third in a series of high-temperature fission product release tests was conducted for 20 min at 2000°C in flowing steam. The test specimen, a 20-cm-long section of H. B. Robinson fuel rod that had been irradiated to ~25,200 MWd/t, was heated in an induction furnace in a hot cell.

Posttest examination showed that the Zircaloy cladding had melted, causing extensive disintegration of the UO_2 fuel and formation of molten phases that appeared to be rich in uranium. Analyses of test components revealed very high fractional releases of ^{85}Kr (59.0%), ^{137}Cs (58.8%), and ^{129}I (35.4%). The releases of ^{125}Sb and ^{110m}Ag, however, were much less than those observed in test HI-2 at 1700°C, perhaps as a result of lower steam flow rate in test HI-3. The extent of aerosol formation, as evidenced by mass of material collected on filters, was similar in the two tests.

CONTENTS

FOREWORD

This document is the third in a series of reports describing the conduct and results of fission product release testing of commercial LWR fuel. Other reports in this series are:

1. M. F. Osborne, R. A. Lorenz, J. R. Travis, and C. S. Webster, Data Summary Report for Fission Product Release Test HI-1, NUREG/CR-2928 (ORNL/TM-8500), December 1982.

2. M. F. Osborne, R. A. Lorenz, J. R. Travis, C. S. Webster, and K. S. Norwood, Data Summary Report for Fission Product Release Test HI-2, NUREG/CR-3171 (ORNL/TM-8667), February 1984.

ACKNOWLEDGMENTS

The authors gratefully acknowledge the significant contributions of several colleagues in conducting this work: D. A. Costanzo, J. Northcutt, and L. Landau of the Analytical Chemistry Division for the ^{129}I determinations and spark-source mass spectrometry; L. Shrader of the Metals and Ceramics Division for metallographic examination; R. P. Wichner and T. B. Lindemer for technical consultation; B. C. Drake for preparation of the manuscript; and M. S. Guy for editing.

LIST OF FIGURES

LIST OF TABLES

DATA SUMMARY REPORT FOR FISSION PRODUCT RELEASE TEST HI-3

M. F. Osborne
R. A. Lorenz
K. S. Norwood
J. R. Travis
C. S. Webster

1. INTRODUCTION

This was the third test in a series designed to investigate fission product release from light-water reactor (LWR) fuel in steam in the temperature range 1400 to ~2400°C.[1] The earlier tests were conducted under similar conditions at temperatures of 500 to 1600°C.[2-5] The purpose of this work, which is sponsored by the U.S. Nuclear Regulatory Commission (NRC), is to obtain the experimental data needed to reliably assess the consequences of heatup accidents in LWRs. The overall objectives of this program are:

1. to determine the extent of fission product release from discharged LWR fuel at temperatures up to and including fuel melting (~2400°C);

2. to identify the chemical forms of the released fission products;

3. to compare the observed fission product behavior with the physical and chemical changes in the fuel specimens;

4. to correlate the results with data from related programs and develop a consistent source-term model applicable to any LWR fuel subjected to a spectrum of accident conditions; and

5. to aid in the interpretation of integral melt tests at ORNL (LWR Aerosol Release and Transport Program) and of tests with simulated fuel only (SASCHA Program at Karlsruhe, Germany).

Tests of fully irradiated LWR fuel are emphasized in this program, but the applicability of simulated fuel (unirradiated UO_2 containing a range of fission product elements) will be investigated in the higher-temperature tests (>2000°C). All tests will be conducted in a flowing mixture of steam and helium (or argon) at atmospheric pressure; steam concentrations will be varied to simulate different accident sequences.

Temperatures in the existing induction furnace will be limited to a maximum of ~2000°C. The currently used ZrO_2 ceramics will be replaced with ThO_2 in the higher-temperature tests. The existing fission product collection and analysis system will be expanded to provide broader sampling capability with the higher-temperature furnace.

This report is intended to provide a brief description of test HI-3 and to tabulate the data obtained. As noted in the previous data summary reports,[6,7] a thorough data evaluation and correlation will be included in

a subsequent topical report covering several fission product release tests.

2. DESCRIPTION OF TEST HI-3

The objective of test HI-3 was to obtain data for fission product release at 2000°C for a period of 20 min in steam flowing at ~0.3 L/min.

2.1 FUEL SPECIMEN DATA

The fuel specimen used in this test was a 20.3-cm (8-in.)-long section from rod H-15 of bundle B05, which operated in the Carolina Power and Light Company's H. B. Robinson 2 Reactor from October 1971 to May 1974.[8] Details of the irradiation and the characteristics of this particular specimen are listed in Table 1; calculated fission product inventories are shown in Tables 2 and 3.

The specimen was cut from section A-8 of the H-15 rod; Fig. 1 shows the location with respect to the gamma-ray profile (which is an indication of the burnup profile). Tapered Zircaloy-2 end caps were pressed onto the ends of the specimen, not to serve as gas seals but to prevent loss of the fractured UO_2 fuel during subsequent handling. A small hole, 1.6 mm (0.063 in.) in diameter, was drilled through the cladding at midlength to serve as a standard leak for gas escape during the heatup phase of the test. These details are illustrated in Fig. 2.

2.2 EXPERIMENTAL APPARATUS

The fuel specimen was heated in an induction furnace (Fig. 3), which was mounted inside a stainless steel containment box in a hot cell (Figs. 4 and 5). This furnace was developed from designs used in previous experimental efforts: fission product release tests,[2-4] fuel rod burst experiments,[9] and molten fuel tests.[10] In test HI-3, the fission product collection system included a platinum thermal gradient tube, fiberglass filters, heated charcoal (for iodine adsorption), and cooled charcoal (for rare-gas adsorption). The steam was collected in a condenser and a dryer, as indicated, prior to reaching the cooled charcoal. Instrumentation included thermocouples and an optical pyrometer for temperature measurement, NaI(Tℓ) radiation detectors connected to a multichannel analyzer, and conventional electrical and gas flow instruments. A data acquisition system (Fig. 6) was used to record test data at 1-min intervals, and several individual chart recorders maintained continuous records of temperatures and flow rates. Differences in apparatus materials and conditions for test HI-3, as compared with the previous tests, are summarized in Table 4.

2.3 CONDITIONS AND OPERATION

The operating conditions of the test are listed in Table 5. Since the hot cell and the experimental apparatus are decontaminated after each test in this series, the apparatus was prepared by direct handling.

Table 1. Data for fuel specimen used in test HI-3

Fuel rod identification	Rod H-15, bundle B05, H. B. Robinson 2 (PWR)
Irradiation data	
Period	October 1971 to May 1974
Maximum linear heat rating, peak (December 1971)	32.6 kW/m (9.95 kW/ft)
Rod average	23.3 kW/m (7.10 kW/ft)
End linear heat rating, peak (May 1974)	21.2 kW/m (6.45 kW/ft)
Rod average	17.5 kW/m (5.34 kW/ft)
Rod fuel loading	2495.4 g UO_2 (2199.6 g U)
Burnup, rod peak	31,000 MWd/t
Burnup, test specimen	25,200 MWd/t
Specimen data	
Length	20.3 cm (8.0 in.)
Location	312 to 332 cm from bottom end of rod
Cladding OD	1.072 cm (0.422 in.)
Specimen fuel loading	136.2 g UO_2 (120.1 g U)
Gas release during irradiation	0.35% of Kr; 0.25% of Xe
Total weight of specimen	167 g
Weight of Zircaloy cladding and end caps	30.7 g

Table 2. Amounts of principal fission and activation product elements in H. B. Robinson fuel specimen HI-3 after 2627 d of decay[a]

Element	Amount in fuel (g/t U)	Amount in specimen[b] (mg)
Se	42.44	5.096
Br	16.42	1.972
Kr	266.6	32.02
Rb	257.9	30.98
Sr	588.3	70.66
Y	335.0	40.23
Zr[c]	2682	322.2
Mo	2539	305.0
Tc	595.5	71.52
Ru	1697	203.8
Rh	378.7	45.48
Pd	1117	134.2
Ag	64.99	7.806
Cd	88.45	10.63
In	2.18	0.262
Sn[c]	73.67	8.847
Sb	17.06	2.050
Te	378.7	45.48
I	187.3	22.50
Xe	4093	491.6
Cs	1878	225.6
Ba	1250	150.1
La	924.3	111.0
Ce	1808	217.0
Pr	848.5	101.9
Nd	3050	366.3
Pm	17.64	2.118
Sm	633.5	76.09
Eu	105.6	12.68
Gd	84.55	10.16
Total of all fission products	26,030	3126
U	9.617×10^5	1.155×10^5
^{235}U	6.857×10^3	8.236×10^2
Pu	7.718×10^3	9.269×10^2

[a]Calculated by C. W. Alexander on May 24, 1982, using the ORIGEN computer program and assuming a burnup of 25.2 MWd/kg and a 2627-d decay to July 15, 1981; adjusted according to the gamma scan of the fuel rod.

[b]Original uranium content of 20.3-cm fuel specimen was 120.1 g; initial enrichment was 2.651% ^{235}U. Thus, the fuel specimen was 120.1 g/10^6 g = 0.01201% of a metric ton (t).

[c]Amounts of zirconium and tin in the Zircaloy cladding were calculated to be 2.086×10^5 and 3.13×10^3 g per (t) of initial uranium, respectively.

Table 3. Principal radionuclides and selected stable nuclides in H. B. Robinson fuel specimen HI-3 after 2627 d of decay[a]

Nuclide	Amount in fuel		Amount in specimen[b]	
	(g/t U)	(Ci/t U)	(mg)	(mCi)
^{83}Kr	31.19	0.0	3.746	0.0
^{84}Kr	83.67	0.0	10.05	0.0
^{85}Kr	11.13	4371	1.337	525.0
^{86}Kr	139.9	0.0	16.80	0.0
^{90}Sr	330.9	45,160	39.75	5424
^{106}Ru	0.969	3246	0.116	389.9
^{110m}Ag	4.77×10^{-4}	2.268	5.73×10^{-5}	0.273
^{113m}Cd	0.151	32.79	0.018	3.938
^{125}Sb	1.921	1984	0.231	238.2
^{129}I	141.8	0.025	17.03	0.0030
^{128}Xe	2.223	0.0	0.267	0.0
^{130}Xe	8.924	0.0	1.072	0.0
^{131}Xe	339.5	0.0	40.77	0.0
^{132}Xe	821.3	0.0	98.64	0.0
^{134}Xe	1120	0.0	134.5	0.0
^{136}Xe	1802	0.0	216.4	0.0
^{134}Cs	7.535	9756	0.905	1172
^{137}Cs	774.8	67,430	93.05	8098
^{144}Ce	0.461	1471	0.055	176.6
^{147}Pm	17.63	16,350	2.117	1964
^{154}Eu	16.41	4431	1.971	532.1
Total	26,030	270,800	3126	32,530

[a]Calculated by C. W. Alexander on May 24, 1982, using ORIGEN computer program and assuming a burnup of 25.2 MWd/kg and a 2627-d decay to July 15, 1981; adjusted according to the gamma scan of the fuel rod.

[b]Original uranium content of 20.3-cm fuel specimen was 120.1 g; initial enrichment was 2.651% ^{235}U. Thus, the fuel specimen was 120.1 g/10^6 g = 0.01201% of a metric ton (t).

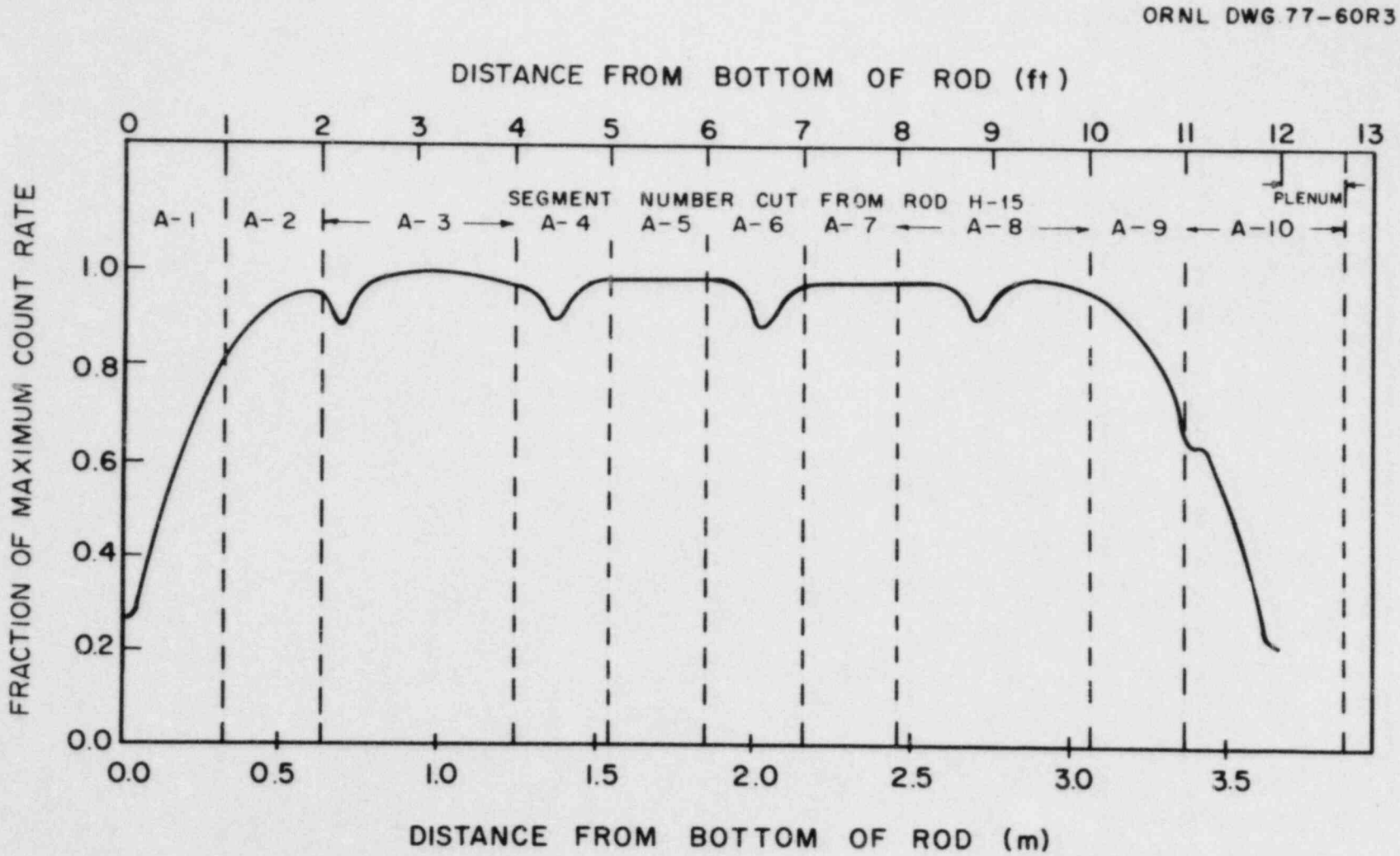

Fig. 1. Gamma profile of fuel rod H-15, showing locations of cuts; section A-9 was used in test HI-3.

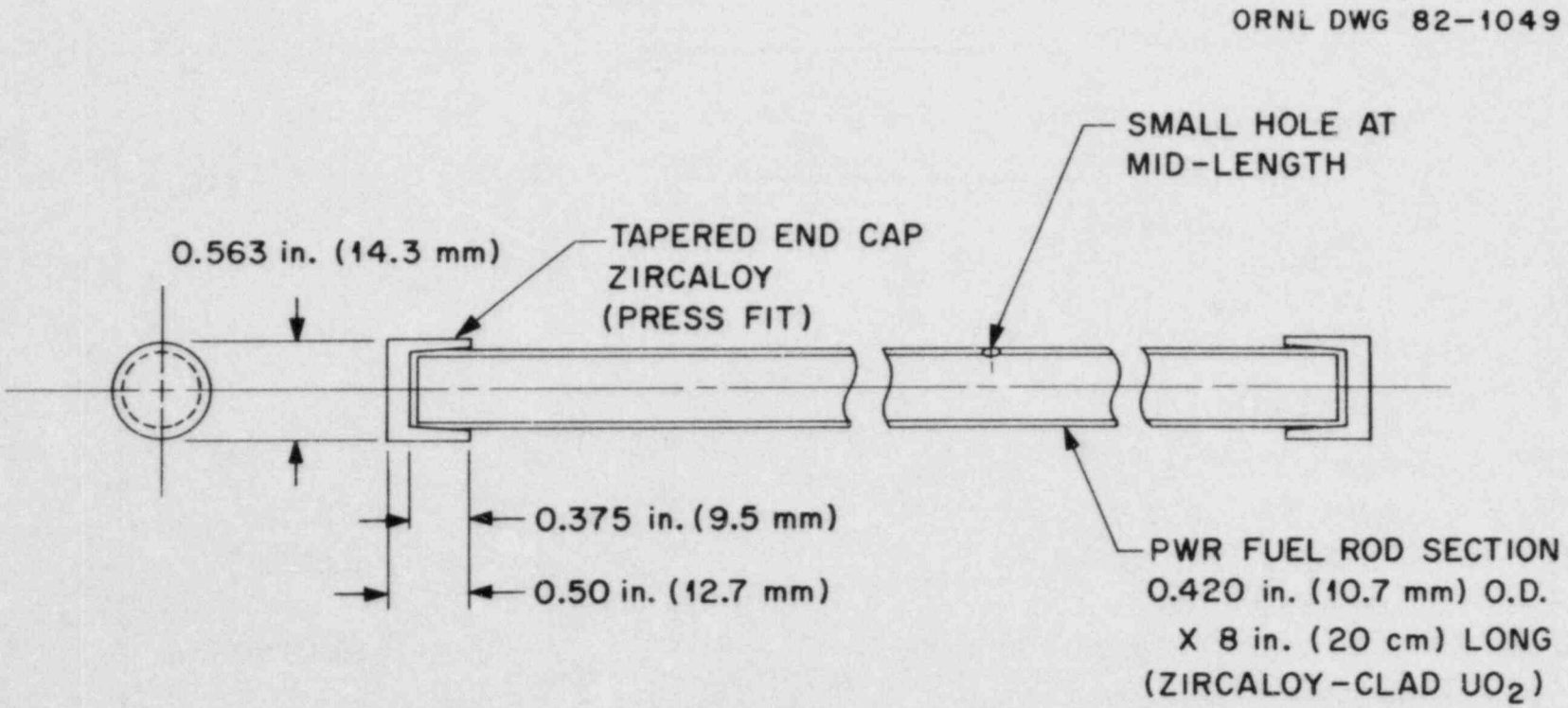

Fig. 2. Fuel specimen for fission product release studies.

ORNL-DWG 81-15401R3

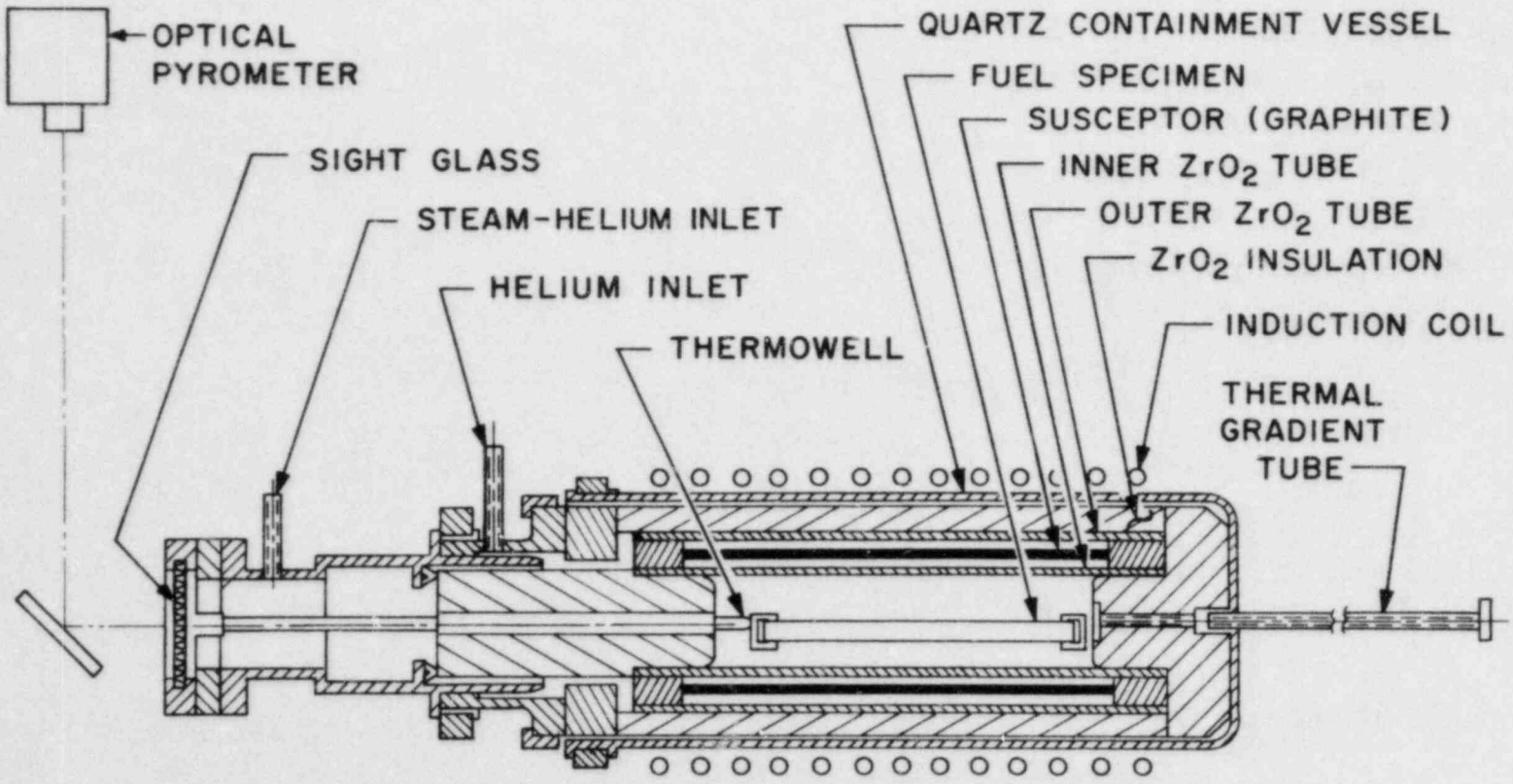

Fig. 3. Fission product release furnace.

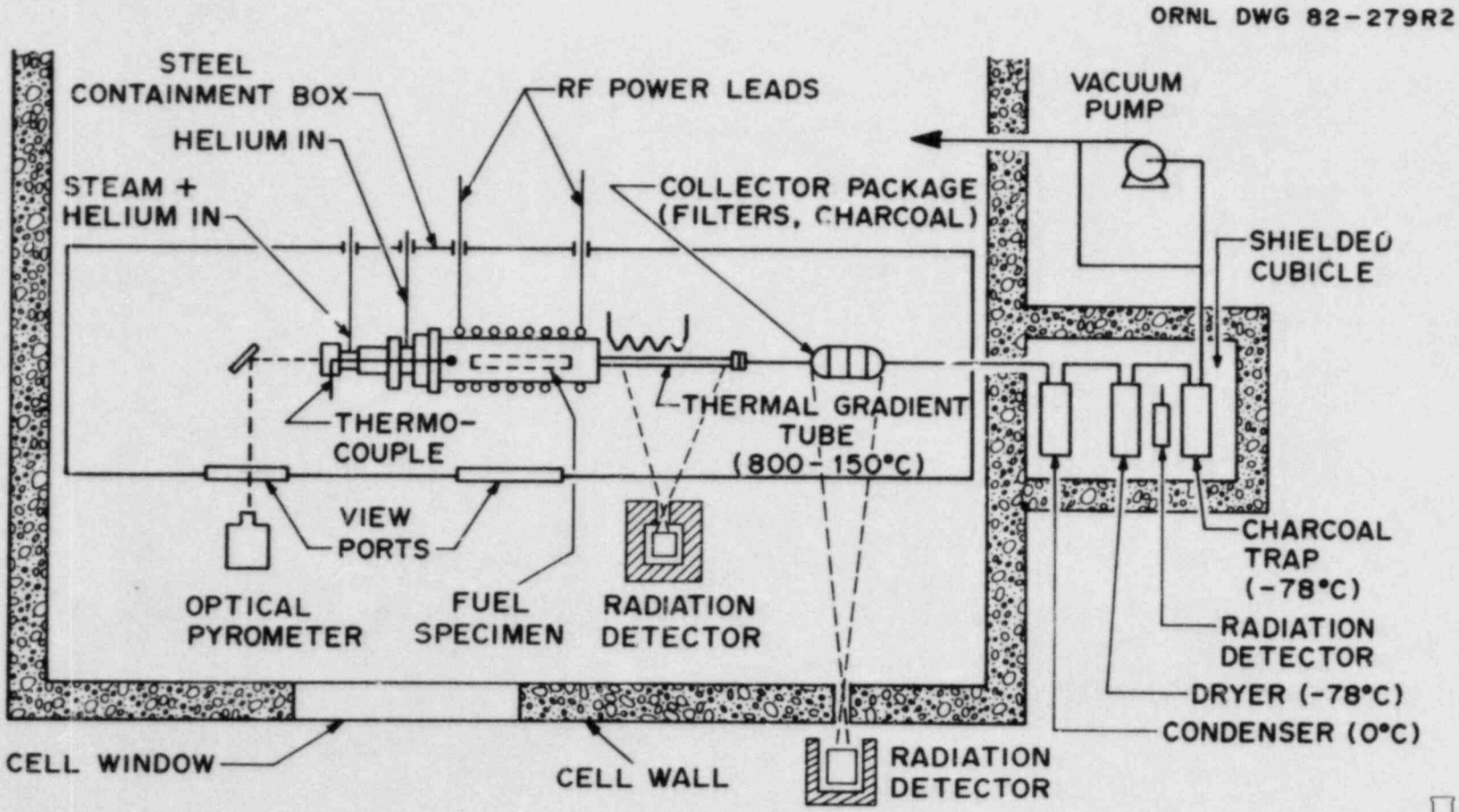

Fig. 4. Fission product release and collection system.

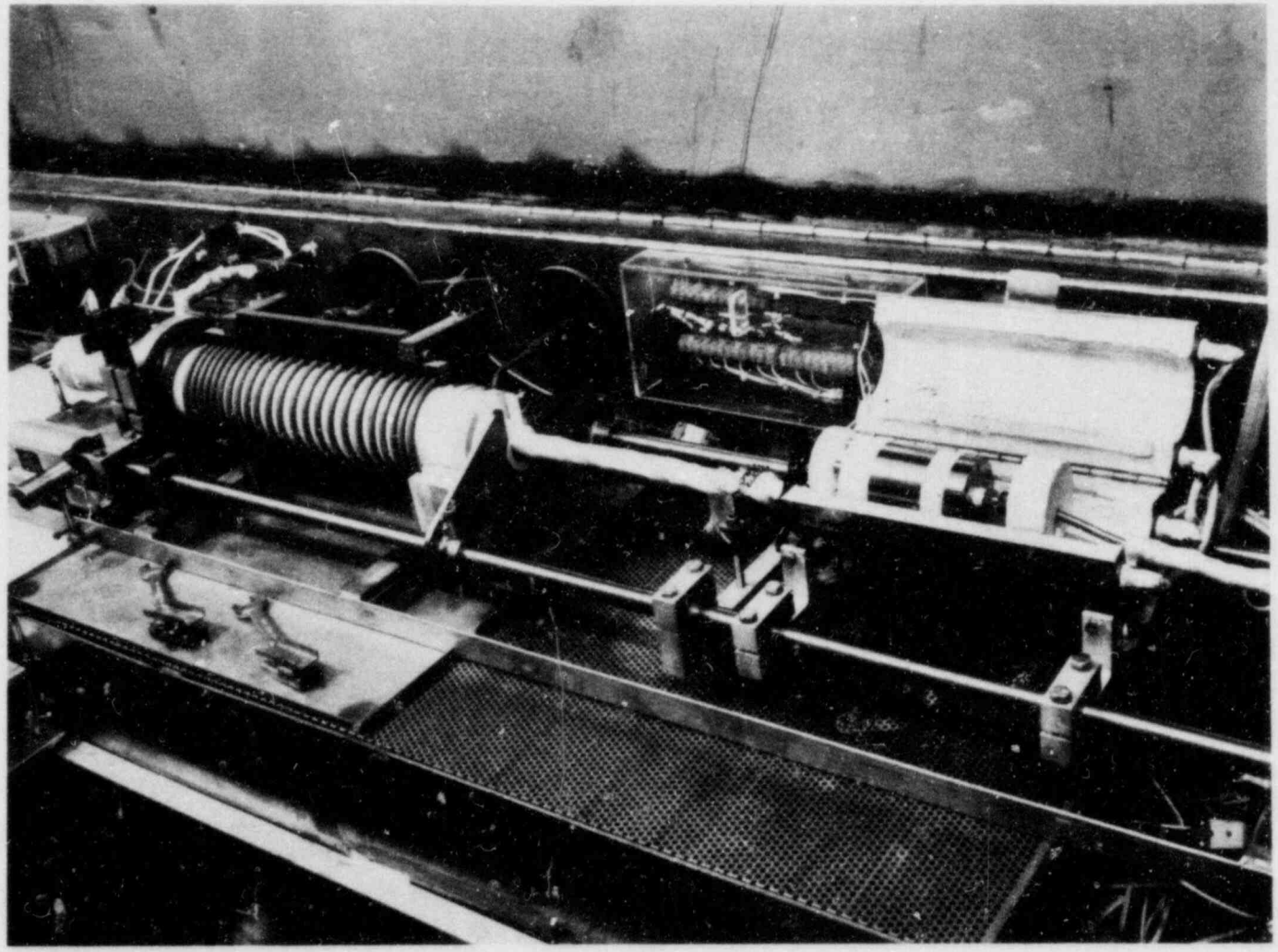

Fig. 5. Photograph of (a) fission product release furnace, (b) thermal gradient tube, and (c) filter package in steel containment box before test HI-3.

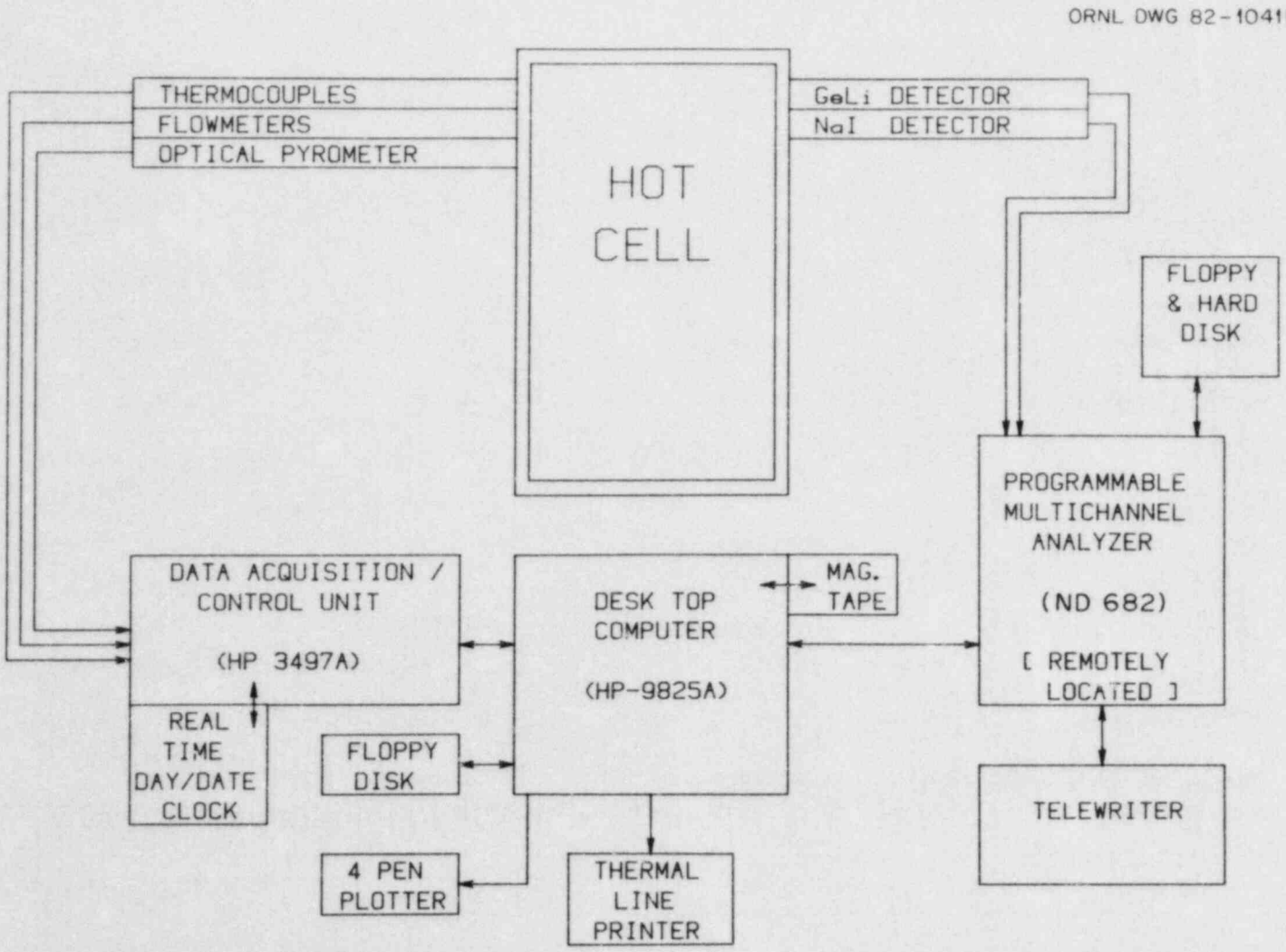

Fig. 6. Data acquisition and processing system for fission product release test.

Table 4. Summary of apparatus and test conditions changed in three tests

Component/condition	Test		
	HI-1	HI-2	HI-3
Furnace thermocouple	Pt-10% Rh vs Pt (bare)	Pt-10% Rh vs Pt (bare)	W-5% Re vs W-26% Re (ZrO_2 thermowell)
Susceptor	Tungsten	Tungsten	Graphite
Pretreatment of fibrous ZrO_2 insulator	None	Zirconyl nitrate (one coat)	Zirconyl nitrate (one coat)
Thermal gradient tube liner	Platinum	Platinum/gold	Platinum
Thermal gradient tube length (cm)	30.5	35.6	35.6
Connector, thermal gradient tube to filter pack	3.2 mm ID × 76 mm long; Teflon	3.2 mm ID × 76 mm long; Teflon	4.6 mm ID × 190 mm long; stainless steel
Entrance cone to filter pack	Teflon	Teflon	Stainless steel
Glasswool prefilter	30 mm diam; Teflon screen	30 mm diam; Teflon screen	51 mm diam; stainless steel screen
Dryer and cold charcoal temperature (°C)	-78	-78	-195
Inert gas	Argon	Argon	Helium

Table 5. Operating conditions for test HI-3

Specimen temperature at start of heatup	250°C
Heatup rate	125°C/min
Nominal test temperature	2000°C
Time at test temperature	20 min
Nominal flow-rate data[a]	
He purge to W susceptor	0.15 L/min
He to steam generator	0.15 L/min
Steam into system	0.3 L/min
Volume flow data[b]	
He purge[c]	11.53 L
He to steam generator[c]	11.14 L
H_2 generated[d]	4.92 L

[a] As measured by mass flowmeters.

[b] As measured by totalizers on mass flowmeters during the 75 min of steam flow into apparatus; operating at room temperature (23°C).

[c] Absolute pressure in furnace during test was 0.1032 MPa (774 mm Hg).

[d] At atmospheric pressure = 0.09975 MPa (748.2 mm Hg).

Master-slave manipulators were used for transferring and loading the highly radioactive fuel specimen, as well as for final closure of the furnace and containment box. No in-cell operations were required during the test. The furnace was preheated in pure helium to ~300°C before steam flow through the system was begun. The rapid heatup was started after the temperatures and flows had stabilized.

2.4 POSTTEST DISASSEMBLY AND SAMPLE COLLECTION

Following the high-temperature test and complete cooldown, the experimental apparatus was disassembled remotely. The filter package and the thermal gradient tube liner were removed first and then transferred to another hot cell to avoid potential contamination from fuel handling. Attempts to remove the fuel specimen from the furnace showed that it was firmly attached to the ZrO_2 furnace tube; in addition, the ZrO_2 end plug immediately downstream from the fuel specimen was immovable. Therefore, we concluded that the extent of cladding melting and/or reaction with the ZrO_2 boat and furnace tube was sufficient to fuse these components together. (Since the melting point of Zircaloy has been reported to be ~1720°C,[11] and pure zirconium melts at ~1850°C,[12] this phenomenon was not a surprise.) The inlet end cap of the fuel specimen, which could be viewed from the furnace inlet, appeared to be intact but heavily oxidized, as expected.

Fusion of the fuel specimen to the ZrO_2 furnace tube required a modified disassembly procedure and prevented direct observation of its condition. The entire unit (ZrO_2 tube, fuel specimen, and end plug assembly) was withdrawn into a glass tube and cast in epoxy resin to preserve the relative orientations during handling and transfer to another hot cell. Upon removal of this assembly from the test cell, it was analyzed for fission product content by gamma spectrometry, and the results were compared with the pretest data. The fuel specimen was then transferred to the High-Radiation Level Examination Laboratory, where it was cut into radial sections for detailed inspection. The highly radioactive components were removed from the hot cell to allow personnel entry for decontamination of the fuel handling area. Then the furnace was completely disassembled, and the components were packaged for gamma-ray analysis. These components typically had about the same level of radioactivity as those in test HI-2.

The filter package and the thermal gradient tube liner were too radioactive for direct gamma-ray spectrometry, even at a distance of 12 m. Therefore, these components were analyzed through 2.54 cm (1 in.) of lead, and the results were adjusted by energy-dependent attenuation factors. The liner of the thermal gradient tube was gamma-scanned at 1.0-cm intervals to determine the distribution of radioactivity (primarily ^{137}Cs) with temperature and then cut into 11 sections based on this distribution. Five smear samples from the liner and one from the prefilter package were collected for mass spectrometric analysis. Each component of the liner and the filter package was analyzed by gamma spectrometry, before and after being leached successively with basic ($NH_4OH + H_2O_2$) and acidic

(HNO_3 + HF) solutions. Iodine release values were obtained by activation analysis of both the solutions and the charcoal from the filter package.

3. TEST RESULTS

3.1 TEST DATA

The temperature and flow data for the entire test, presented in Fig. 7, are uncorrected; pretest temperature calibrations showed that the average temperature of the fuel specimen should have been 100 to 150°C above that indicated by the thermocouple and the optical pyrometer values, both of which detect the temperature at the gas inlet end of the furnace. The operating conditions for test HI-3 are summarized in Table 5. Based on the flow data (steam in and hydrogen out), at least one-third of the Zircaloy cladding was oxidized to ZrO_2 during the test (note the peak in total flow out at 14 min in Fig. 7). Posttest examination confirmed complete disintegration of the fuel specimen, apparently the result of clad melting, UO_2 dissolution, and severe oxidation. The release histories of ^{85}Kr to the cold charcoal traps and of ^{137}Cs to the thermal gradient tube and the filters are related to test temperatures in Fig. 8. These values were determined as relative rates during the test, and quantitative measurements with a multichannel analyzer after the test were used to determine fractional releases. The monitor for the thermal gradient tube viewed only the lower-temperature end of the tube. Significant release during specimen cooling is apparent from the release curves.

3.2 POSTTEST DATA

After the test apparatus was disassembled, each component was analyzed by gamma-ray spectrometry to determine the amounts of the gamma-radioactive species present. (As noted previously, ^{137}Cs and ^{134}Cs comprised most of the gamma activity in the fuel; these high levels of cesium interfered with analyses for the less abundant and less radioactive fission products.) The fractional release results for various system components are summarized in Table 6; the fission products remaining in the test specimen are discussed in Sect. 3.2.6.

3.2.1 Results from Gamma Spectrometry

The detailed results of gamma spectrometric analyses for ^{137}Cs are contained in Table 7. As expected, large amounts of cesium had migrated to regions where rapid condensation was possible. Approximately half of the cesium that escaped from the furnace was collected on the filters, indicating its association with particulate material. The distribution of cesium throughout the test apparatus is illustrated in Fig. 9; the iodine distribution, as determined by component leaching and activation analysis for ^{129}I, is included for comparison. These curves show the much higher levels of cesium as compared with iodine at most locations, reflecting the higher inventory of cesium (see Table 2). As in tests HI-1 and HI-2, a high concentration of cesium occurred at the furnace outlet, indicating condensation (and possibly chemical reaction) on the ZrO_2 end plug at

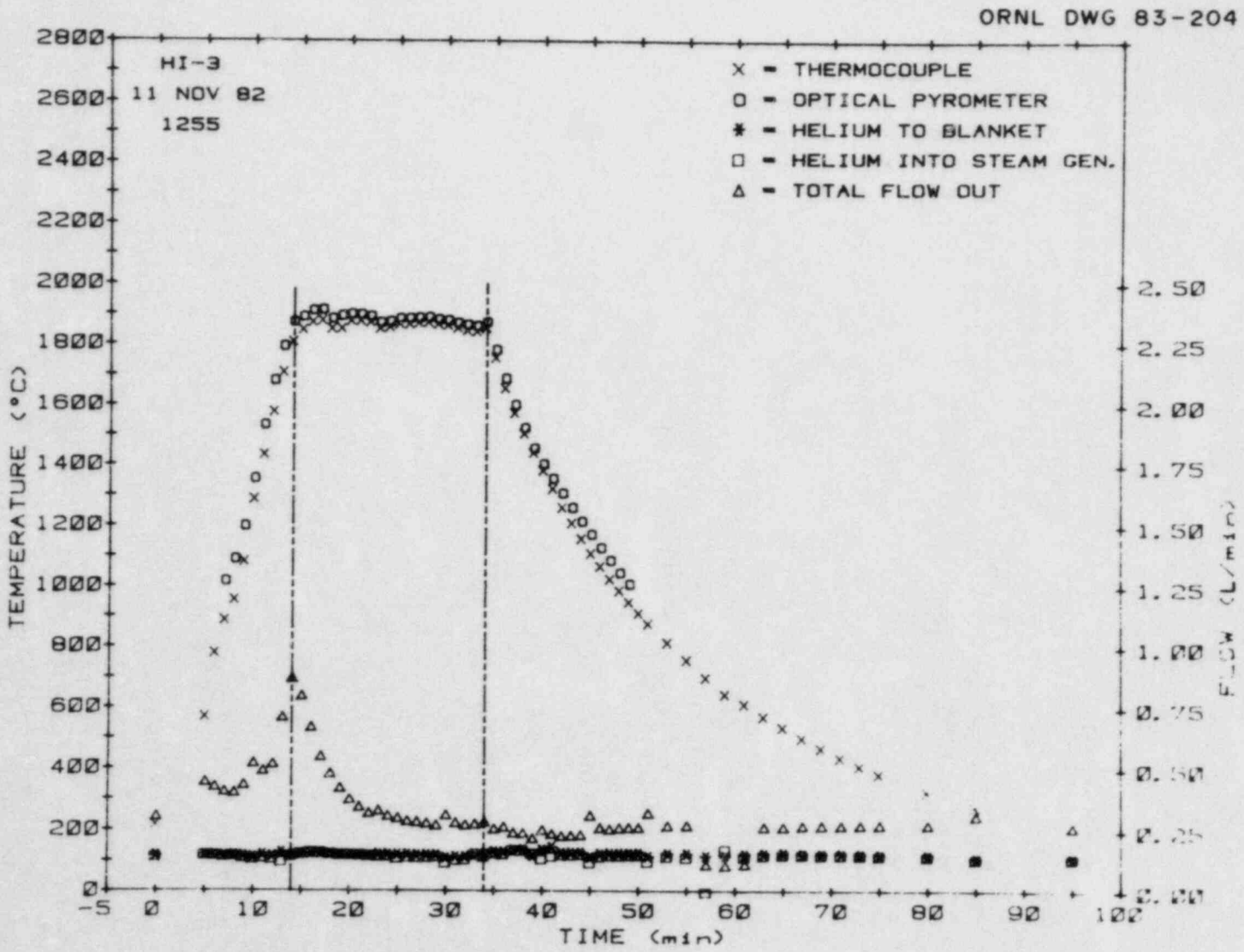

Fig. 7. Temperature and flow history of test HI-3. Note peak in total flow out at 14 min, indicating H_2 generation from steam-Zircaloy reaction.

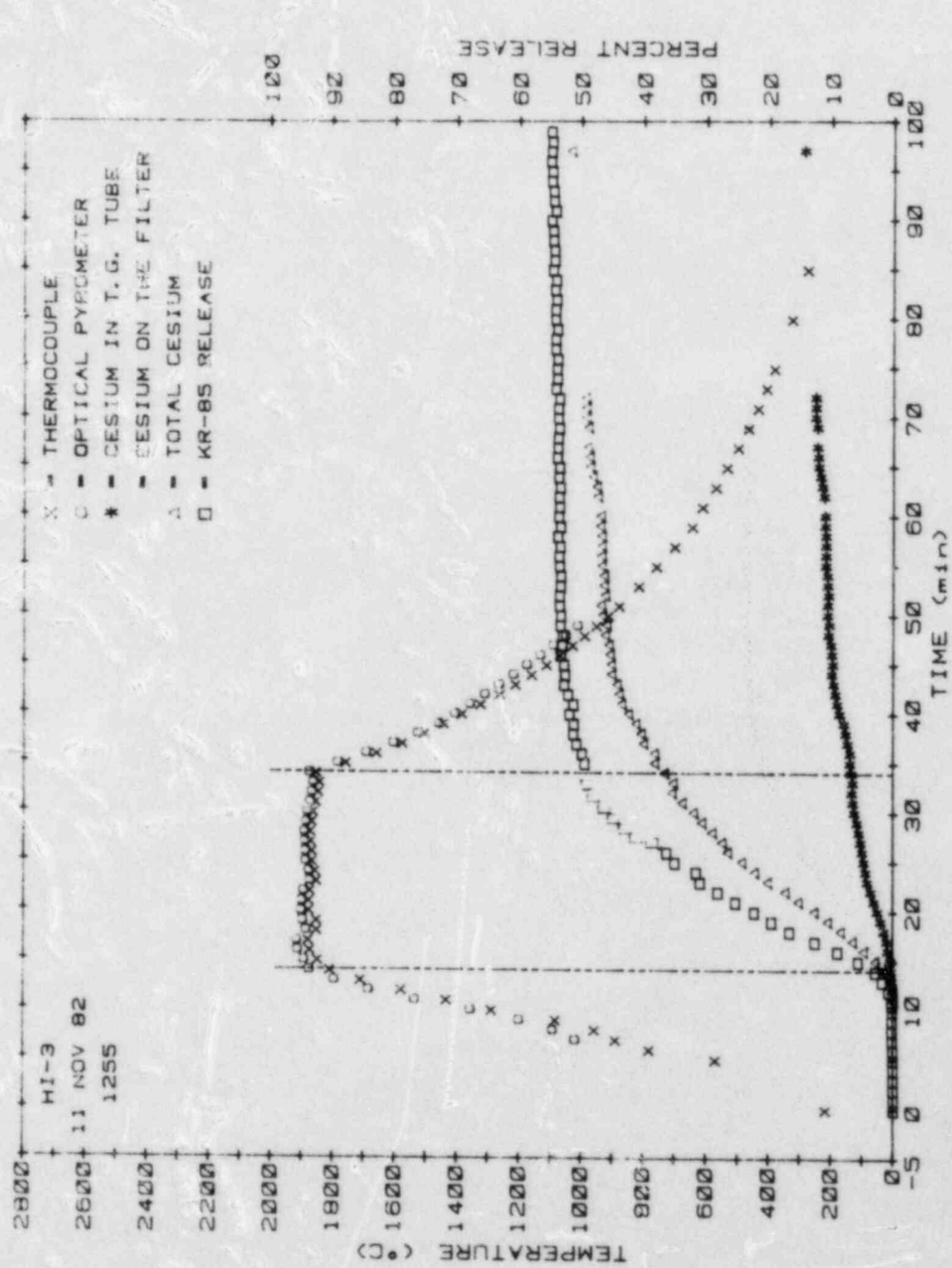

Fig. 8. Release of ^{85}Kr and ^{137}Cs as functions of temperature and time in test HI-3.

Table 6. Distribution and fractional release of fission products in test HI-3

Test component or collector	Temperature or range (°C)	Fraction of specimen inventory found on test components (%)				
		^{85}Kr	^{137}Cs	^{129}I	^{125}Sb[a]	^{110m}Ag[a]
Furnace[b]	2000–1000	0	14.6	0.60	10^{-3}	0.015
Thermal gradient tube	900–140	0	15.7	12.4	0	0
Filters	140	0	28.5	22.4	0	0
Hot charcoal	140	0	10^{-7}	10^{-3}	0	0
Cold charcoal	-196	59.0	0	0	0	0
Total		59.0	58.8	35.4	10^{-3}	0.015

[a]Because of the high levels of cesium activity, ^{125}Sb and ^{110m}Ag could not be detected on most components. Based on past experience, small amounts were probably present in other locations, especially on the thermal gradient tube.

[b]Fuel specimen could not be removed from the ZrO_2 furnace tube and the end plug; therefore, some released material remained with these components and could not be analyzed separately.

Table 7. Distribution of cesium in test HI-3

Location	Temperature (°C)	Cesium found in each location: Amount (μCi ^{137}Cs)	Amount (mg total Cs)	% of specimen inventory[a]	% of released
Furnace components					
Inlet end components	~1000	3.709+2[b]			
Outer ZrO_2 tube	2000	8.681+2			
Fibrous ZrO_2 insulator	1000–1800	1.699+3			
Graphite susceptor	2100	1.797+3			
Outlet end components	1000–1500	1.876+5[c]			
ZrO_2 outlet end plugs	1000–2000	9.46+5[c]			
Miscellaneous debris	800–2000	8.662+3			
Quartz vessel	~800	3.657+4			
Total		1.18+6	32.87	14.57	24.79
Thermal gradient tube					
Quartz tube	1000–140	2.803+5			
Pt segment 1	750	1.071+5			
Pt segment 2	800	4.043+3			
Pt segment 3	720	4.768+4			
Pt segment 4	650	2.404+5			
Pt segment 5	580	2.750+5			
Pt segment 6	520	1.857+5			
Pt segment 7	460	9.057+4			
Pt segment 8	390	1.079+4			
Pt segment 9	330	6.371+3			
Pt segment 10	260	6.605+3			
Pt segment 11	180	1.184+4			
Wipe from push rod		4.201+3			
Total		1.271+6	35.41	15.70	26.70
Filter package	~140				
Entrance tube		4.423+4			
Entrance cone		1.754+3			
Glass wool prefilter		2.222+6			
First HEPA filter		3.708+4			
Second HEPA filter		4.429+2			
Heated charcoal		7.27-3			
Miscellaneous parts		2.[illegible]7+2			
Total		2.[illegible]9+6	64.33	28.51	48.51
Other components					
Condenser		[illegible]-2			
Dryer	-196	3.96-2			
Cooled charcoal	-196	0			
Total		5.20-2	1.4-6	6.4-9	1.1-8
Total all components		4.76+6	132.6	58.78	100

[a]Based on average burnup of 25.2 MWd/kg, the test specimen contained 225.6 mg of cesium and 8.098 Ci of ^{137}Cs (= 2.786-5 mg Cs/μCi ^{137}Cs); decay corrected to July 15, 1981 (ORIGEN calculation).

[b]Exponential notation: 3.709+2 = 3.709×10^2, etc.

[c]Counted through 1.0 or 1.5 in. lead because of high radioactivity and corrected for attenuation.

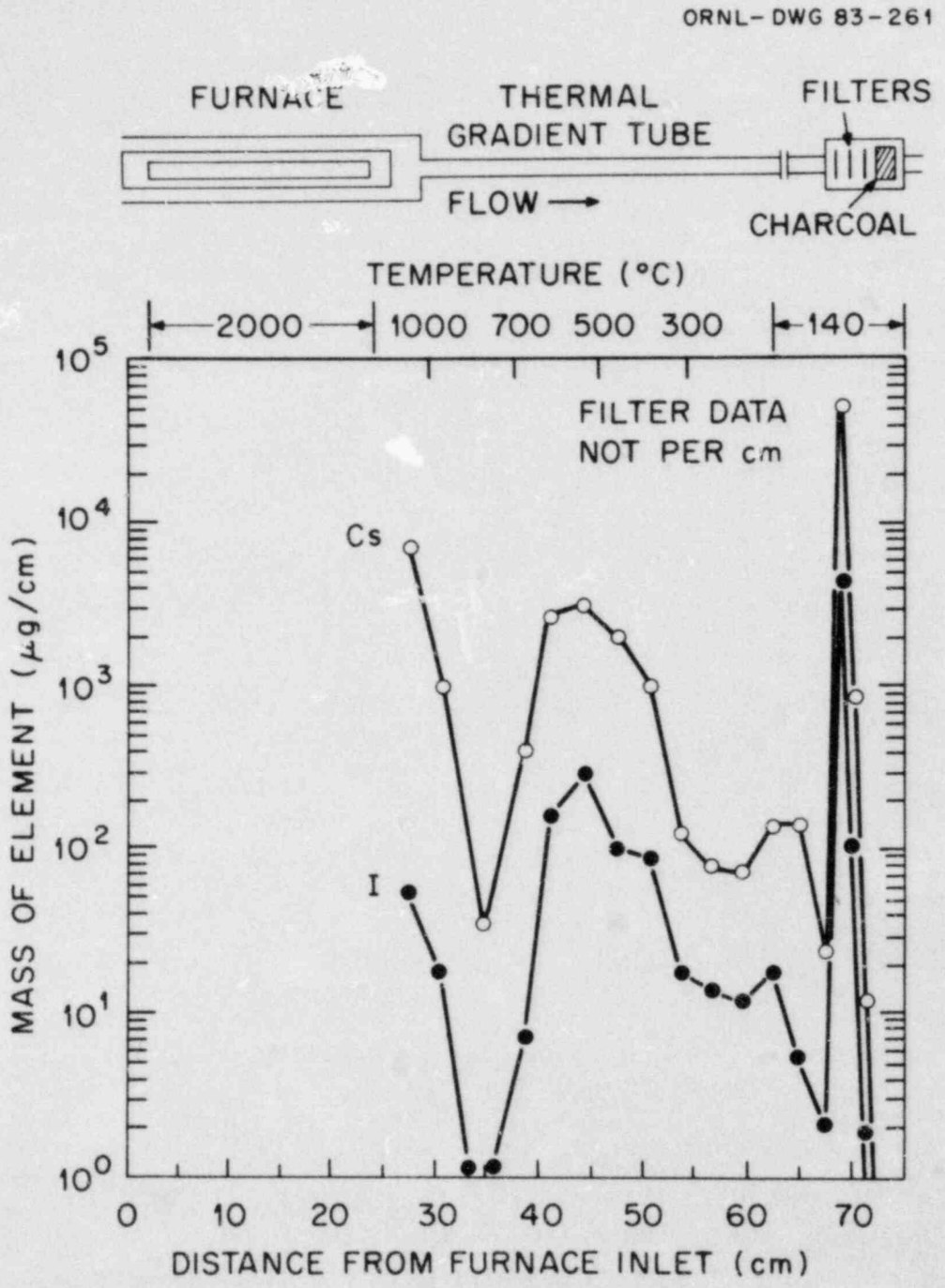

Fig. 9. Distribution of cesium and iodine in test HI-3.

~1200°C. Because the fuel could not be removed from the ZrO_2 furnace tube, we were not able to determine the amount of cesium on that component.

The basic solution that was used as a leachant to remove iodine from the test components also removed a large fraction of the cesium. The results of leaching the thermal gradient tube sections will be discussed in Sect. 3.2.5. Unlike the components from earlier tests, however, very little ^{125}Sb or ^{110m}Ag was detected, even after removal of more than 99% of the ^{137}Cs. Thus, we conclude that the fractional releases of antimony and silver from the furnace to the collection system were lower than in test HI-2. Further attempts to detect antimony, silver, and tellurium in the cladding and the furnace are under way.

3.2.2 Results of Activation Analysis for Iodine

Since iodine has no long-lived, gamma-emitting nuclides, neutron activation analysis was used to measure iodine on selected components, especially the thermal gradient tube. Iodine forms dissolve readily in basic solutions to form stable iodides; in our samples, large amounts of highly radioactive cesium were also dissolved. Small aliquots of the solutions were chemically treated to remove cesium prior to being irradiated; then the 12.4-h ^{130}I was counted. The results of these analyses, along with the data on fractional iodine release and the cesium/iodine ratios at various apparatus locations, are summarized in Table 8. The very small amounts of iodine on the second HEPA filter and the heated charcoal show that a very small fraction (<0.01%) of the iodine was of a form that penetrated the first two filters. The total fraction of iodine released, 35.4%, is actually a minimum value; some iodine may have gone undetected because (1) iodine cannot be detected directly and (2) it is impossible to leach and sample all surfaces of the test apparatus. The heated charcoal was also analyzed (by activation) for bromine, which should behave similarly to iodine; 0.22 μg was detected, corresponding to ~0.01% of the specimen inventory.

3.2.3 Results of Spark-Source Mass Spectrometric Analyses

Spark-source mass spectrometry (SSMS) is used to obtain data for a broader range of elements since only a limited number of the elements that may be released from the furnace to the collection system can be measured by gamma spectrometry. Because of the nature of the analyses and the sampling techniques, this method is less precise (accuracy estimated to be a factor of ~3); however, we did obtain data for several important elements that were not available otherwise.

In test HI-3, SSMS smear samples were taken from five locations along the liner of the thermal gradient tube and from the glass wool prefilter. (These samples are taken by touching the tip of a small graphite electrode to the sample location; a microscopic amount of the deposited material adheres to the graphite electrode and is subsequently vaporized in the mass spectrometer.) The results of these analyses, which are summarized

Table 8. Fractional release and distribution of iodine in test HI-3 (results of activation analysis for ^{129}I)

Location	Temperature (°C)	Iodine found at each location: Amount (μg ^{129}I)	Amount (μg total I)	Percentage of specimen inventory[a]	Percentage of total I released	C/I ratio (μg Cs/μg I)
Furnace components						
Quartz vessel	~800	68.3				11.3
ZrO_2 ceramics	~1000	33.7				534
Total[b]		102.0	134.8	0.60	1.70	225
Thermal gradient tube						
Quartz tube (all)	1000–140	68.4				86.5
Segment 1	750	42.6				53.1
Segment 2	740	0.63				135.0
Segment 3	680	21.1				47.7
Segment 4	600	349				14.5
Segment 5	510	660				8.79
Segment 6	440	624				6.28
Segment 7	380	201				9.51
Segment 8	320	38.6				5.90
Segment 9	270	31.5				4.67
Segment 10	220	27.0				5.16
Segment 11	160	41.5				6.02
Total		2105	2780	12.36	34.97	12.74
Filter pack						
Entrance tube	140	77.5				12.0
Entrance cone	140	1.61				23.0
Glass wool filter	140	3340				14.0
First HEPA filter	140	82.1				9.53
Second HEPA filter	140	1.46				6.40
Charcoal	140	0.16[c]				2.9-4
Miscellaneous parts	140	306				0.23
Total		3810	5030	22.36	63.27	12.79
Total all components		6020	7950	35.33	100	16.36

[a]Based on an average burnup of 25.2 MWd/kg, the test specimen contained 17.03 mg of ^{129}I and 22.50 mg of total iodine; decay was corrected to July 15, 1981.

[b]Small amounts of iodine probably were present on other furnace components that were not leached.

[c]In addition, 0.22 μg of bromine was found on the charcoal; this value corresponds to 0.011% of the specimen inventory as compared with 0.001% of the iodine found on the charcoal.

in Table 9, are based on either the amount of ^{137}Cs, as measured by gamma spectrometry, or on a known quantity of erbium, which was added as a standard. The data in Table 9 are divided into three groups: (1) fission products; (2) special materials, such as fuel (U), cladding (Zr and Sn), and apparatus structural materials (Zr, Ca, Mg, and Pt); and (3) other materials, which are impurities in the system. Selected data from this table are plotted in Fig. 10 to illustrate the distribution along the thermal gradient tube. These curves show that the distributions of cesium and iodine peak near the midlength of the tube; however, the total fission products and other materials reach peak concentrations near the inlet, which operated at a much higher temperature. With the exception of a large value for silver (which probably did not result from fission in this case), no significant amount of fission product material was found at the 5-cm position, where the other materials were most concentrated. As shown in Table 9, the cesium/rubidium ratio was ~4 in the SSMS samples; since the ratio in the fuel was 7.28 (Table 2), this suggests that rubidium was released in a higher fraction than was its dominant chemical analog cesium. Note, however, that the expected accuracy of measurement is only a factor of 3. The sparse data for the chemical analogs iodine and bromine seemed to agree. Compared with test HI-2, relatively little tellurium and silver were detected. As evidenced by the relative fractions that passed through the thermal gradient tube to the filters, the fission products were more volatile than the other materials. Some of the nonfission products originate from the ZrO_2 ceramics; calcium or magnesium oxides are mixed in the ZrO_2 (~5 wt %) as stabilizers, and the released bismuth and lead apparently result from low-level (<0.1 wt %) ThO_2 impurity. As noted in the report of test HI-2,[7] we suspect that these SSMS analyses indicate a number of element identifications that are artifacts of sampling and handling rather than relevant test data.

3.2.4 Mass of Material Collected on the Thermal Gradient Tube and Filters

Significant aerosol formation is typically observed in high-temperature experiments of this type, especially under conditions causing chemical reaction. Appreciable deposits were noted on the thermal gradient tube and the prefilter in both tests HI-1 and HI-2, but no direct measurements of the masses were made. In test HI-3, pretest and posttest weights of these components were obtained; the appearance of the filters is shown in Fig. 11. These data, along with estimates of the comparable values for the earlier tests (based on SSMS and gamma spectrometric results) and estimates of the aerosol concentrations in the flowing gas, are shown in Table 10. Although some of the material deposited on the collectors directly from the vapor phase, no distinction was considered in the estimation of aerosol concentrations. In addition, some of the elements occur as impurities from the apparatus with no direct relation to a fuel aerosol.

Table 9. Results of spark-source mass spectrometric analyses of samples from test HI-3

Element	Mass of element found					
	Thermal gradient tube sample (mg/cm)					Filter-1 (mg total)
	1	2	3	4	5	
Distance from inlet (cm)	0.5	5	12	21	30	
Fission products						
Cs (R)[a]	0.869	0.029	1.50	1.19	0.062	61.9
Rb (R)	0.21	0.008	0.55	0.28	0.009	17.3
I (R)	0.11		0.16	0.31	0.021	17.3
Br (R)	0.021			0.031	0.005	0.58
Te (R)	0.032			0.001	0.003	0.12
Ag (?)		1.4[b]	0.031	0.0003	0.005	0.58
Cd (?)	0.32		2.2	0.13	0.07	11.5
Total	1.56	1.44	4.39	1.94	0.178	109
Special materials[c]						
Sn (N)	0.032	1.1	0.79	0.22	0.008	0.58
Zr (N)				0.002	0.001	0.02
Ca (N)	0.021	0.19	0.039	0.001	0.001	0.06
Mg	0.75	0.81	<0.016	0.022	0.053	~17.0
U				0.006	0.008	
Pt	1.1	5.4	7.9	0.22	0.006	
Total[d]	0.803	2.10	0.845	0.251	0.071	~17.7
Other materials[e]						
Bi	0.11	2.7	0.047	0.003	0.075	5.8
Pb	0.11	0.27	0.16	0.006	0.032	5.8
Zn	0.043	1.1		0.002	0.002	0.12
Cu		<0.03	0.016		0.001	0.04
Ni	0.053	0.19	0.071	0.003		<0.005
Co		0.027	0.016	0.002		
Fe	0.011	0.54	0.24	0.006	0.011	0.06
Mn	0.004	0.19		0.002		0.06
Cr	0.021	0.27	0.047			0.02
K	0.021	0.027	0.024	0.006	0.001	0.58
Cl	0.11	2.7	0.39	0.031	0.003	1.2
S	0.75	1.9	3.2	0.31	0.053	28.8
P	0.054	0.054	0.008			0.06
Al	0.011	0.054	0.016	0.002	0.001	0.02
Na	0.064	0.027	0.008	0.002	0.004	2.9
Total	1.36	10.1	4.24	0.375	0.183	45.5
Total all materials	3.72	13.6	9.48	2.57	0.432	172

[a](R) denotes radiogenic isotopic distribution, (N) denotes natural isotopic distribution, and (?) denotes mixture or uncertain isotopic distribution.

[b]Probably not fission product.

[c]Material known to be part of the system, such as fuel, cladding, and apparatus structural materials.

[d]Excluding platinum, the deposition surface.

[e]Apparently impurities in system.

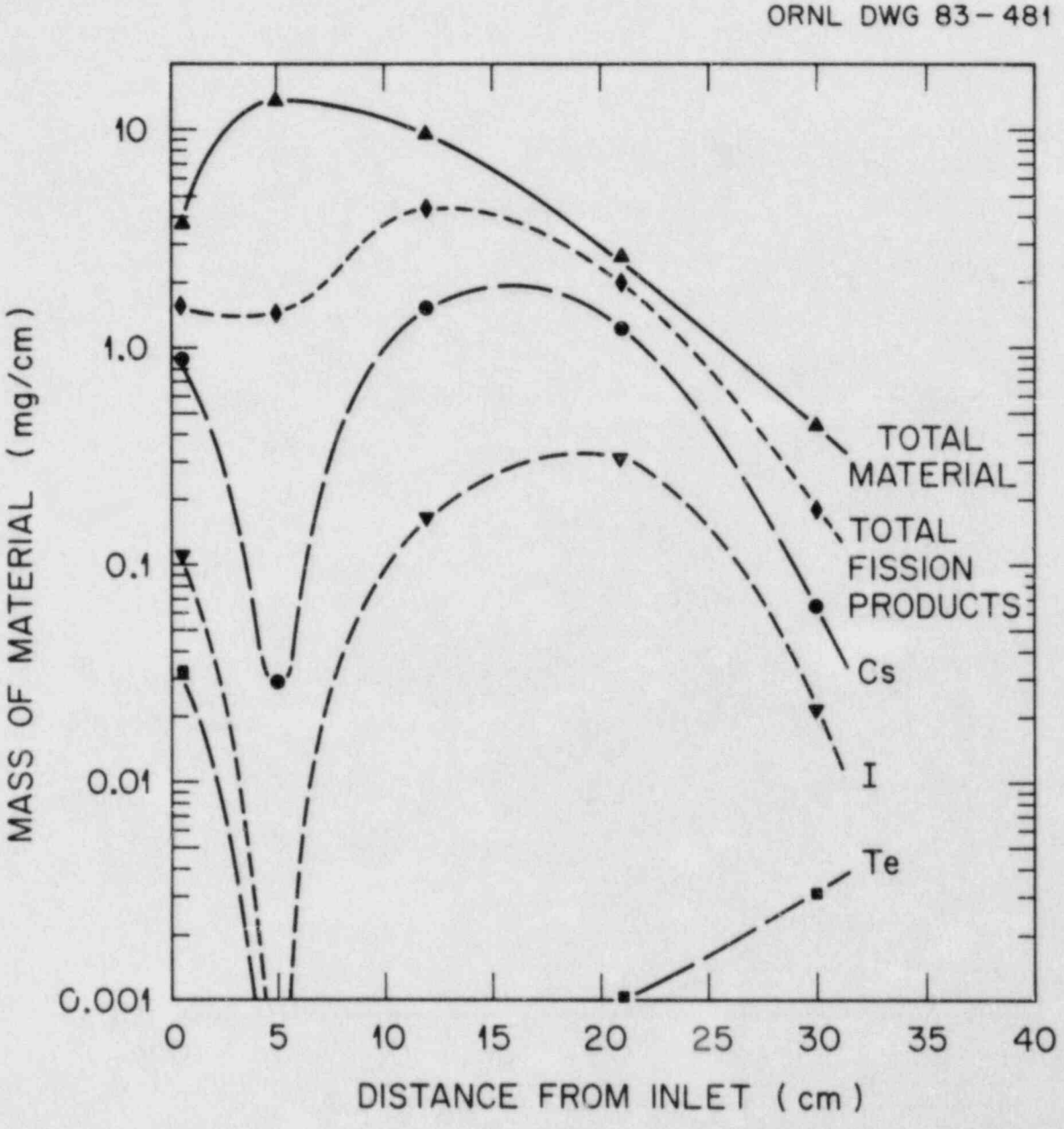

Fig. 10. Distribution of fission products and total deposited material in test HI-3 thermal gradient tube, as indicated by SSMS analyses.

Y-188458

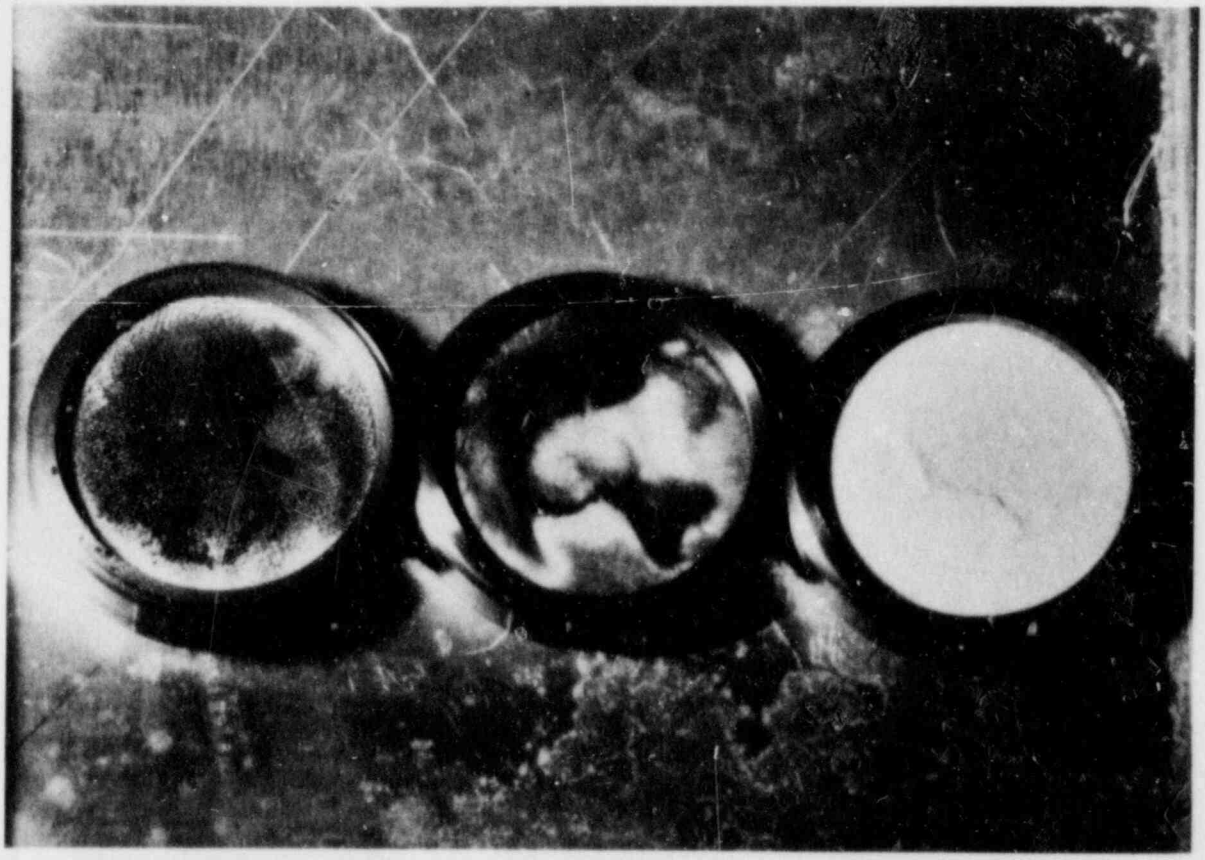

Fig. 11. Appearance of filters from test HI-3; from the left, screen covering glass wool prefilter, first HEPA, and second HEPA.

Table 10. Aerosol produced in fission product release tests

Test	Temperature (°C)	Mass collected on thermal gradient tube (mg)	Mass collected on filter (mg)	Aerosol concentration[a] (g/m^3)	
				At furnace temperature	At 100°C
HI-1[b]	1400	~5	~18	<0.1	~0.4
HI-2[c]	1700	~70	~230	~1.6	~7.0
HI-3[c]	2000	80	220	2.5	15.0

[a]Assumes test time plus 5 min for aerosol production time.

[b]Mass of deposits estimated from mass spectrometric data.

[c]Mass of deposits determined by weighing thermal gradient tube and filters.

3.2.5 Thermal Gradient Tube Results

The thermal gradient tube, 0.4 cm in internal diameter and made of quartz, was lined with platinum foil to provide an inert deposition surface. When the furnace was at high temperature, the thermal gradient tube cooled the in-flowing gas; the heat was rejected by conduction, radially in the gas and then through the platinum liner, a small gas gap, and the quartz tube. Thermocouples on the outside of the quartz measured the temperature, and four heaters preheated the tube and controlled the gradient during the test. Appendix A contains a crude calculation of the radial temperature distribution; the results at steady state may be summarized as follows:

1. thermocouple temperature = x K,
2. inside surface of the platinum = x + 6 K, and
3. center gas temperature = x + 21 K.

Figure 12 shows the measured thermocouple temperatures during the 20 min while the fuel was at 2000°C. The error bars represent the mean ±1 standard deviation; the temperatures varied as the gas enthalpy and gas composition changed during the experiment.

Table 11 summarizes the cesium and iodine data for the thermal gradient tube. The cesium profile (plotted in Fig. 13) shows an accumulation

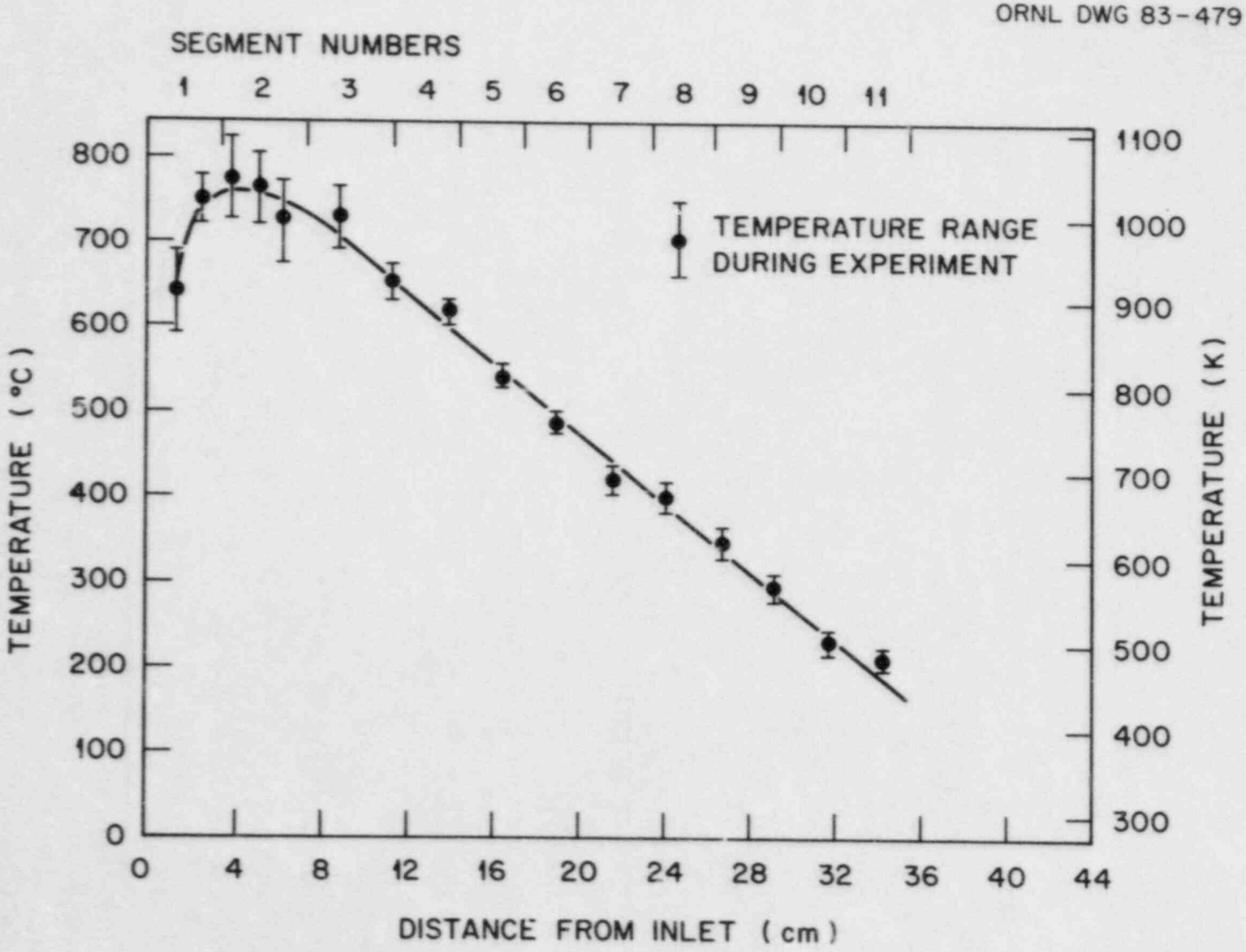

Fig. 12. Temperature distribution along thermal gradient tube in test HI-3.

Table 11. Cesium and iodine on HI-3 thermal gradient tube

Position (cm)	Temperature[a] (K)	^{137}Cs[b] (mCi)	Cs[c] ($\mu g/cm^2$)	^{129}I (μg)	I[d] ($\mu g/cm^2$)
0–4	890–1050	110	780	43.0	15.0
4–8	1010–1050	4	30	0.63	0.22
8–12	930–1010	47	350	21.0	7.4
12–15	870–930	240	2300	350	160
15–18	810–870	270	2700	660	310
18–21	750–810	180	1800	620	290
21–24	690–750	90	880	200	94.0
24–27	620–690	11	110	39.0	18.0
27–30	560–620	7	69	31.0	15.0
30–33	500–560	6.6	65	27.0	13.0
33–36	420–500	12	120	42.0	19.0

[a]Temperature of deposition surface (platinum).

[b]Counted after sectioning; allowance made for air attenuation of 662-keV gamma ray of ^{137}Cs; decay corrected to July 15, 1981.

[c]ORIGEN calculation gives specific activity of cesium as 35.9 Ci of $^{137}Cs/g$ on July 15, 1981.

[d]ORIGEN calculation gives ^{129}I as 75.7% of total iodine on July 15, 1981.

of cesium at the inlet and a single large peak beginning at a deposition surface temperature of 1040 K (770°C) and peaking at 870 K (600°C); there was a slight accumulation at the exit. Of the cesium that entered the tube, 38% deposited and 62% escaped and was trapped on the filters downstream.

Figure 14 shows the iodine profile plotted from Table 11. It follows the cesium profile very closely, showing a peak beginning at a deposition surface temperature of 1040 K (770°C) and peaking at 830 K (560°C). Of the iodine that entered the thermal gradient tube, 35% deposited and 65% escaped and was trapped by the downstream filters.

3.2.5.1 Interpretation: Cesium and Iodine on the Thermal Gradient Tube

The peaks in the iodine and cesium profiles are narrower than those in tests HI-1 and HI-2. We attribute this to the lower gas velocity (about half that in HI-1 or HI-2); molecules diffusing to the walls were not transported as far down the tube, and the peaks in the profiles were not broadened.

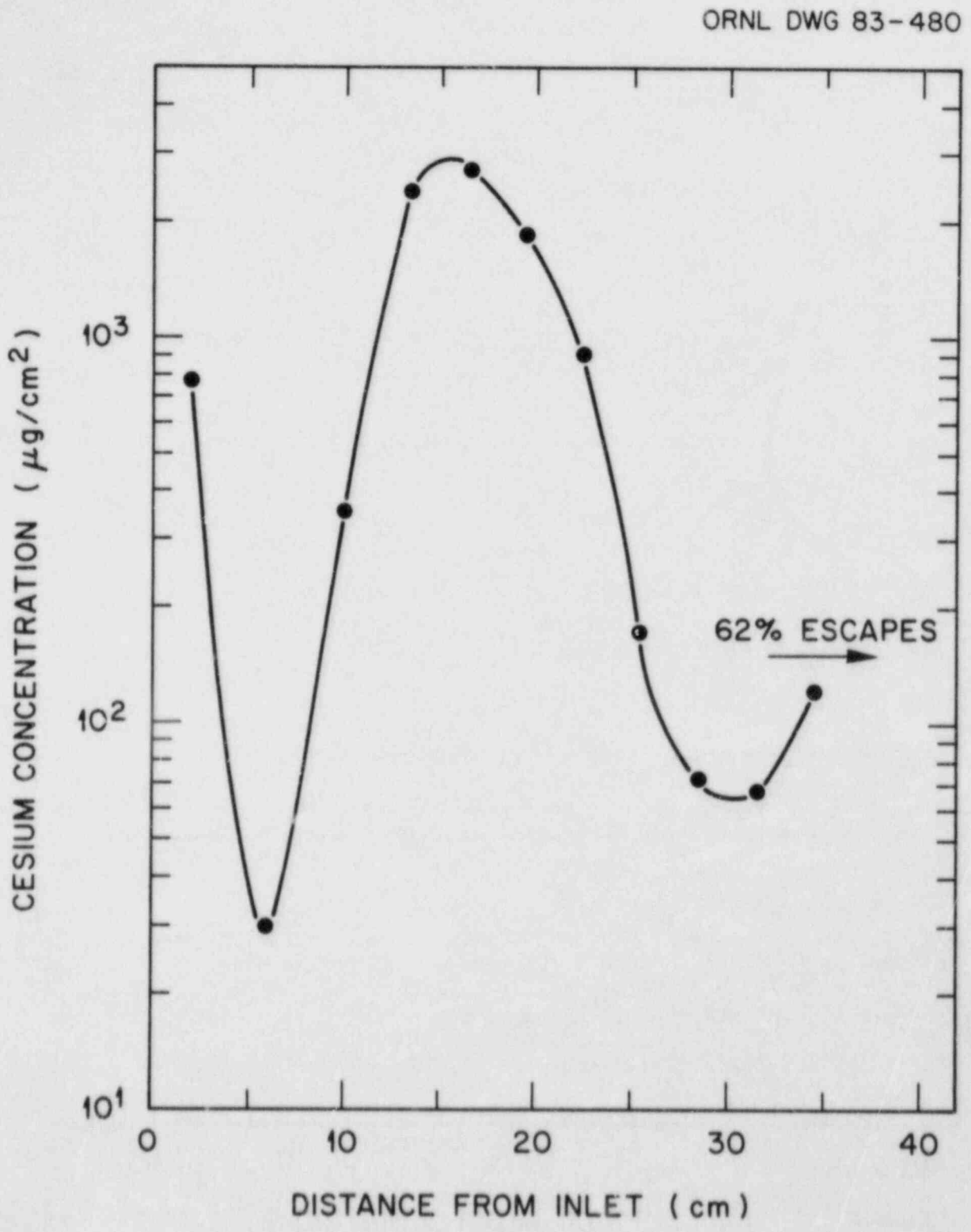

Fig. 13. Distribution of cesium in thermal gradient tube in test HI-3.

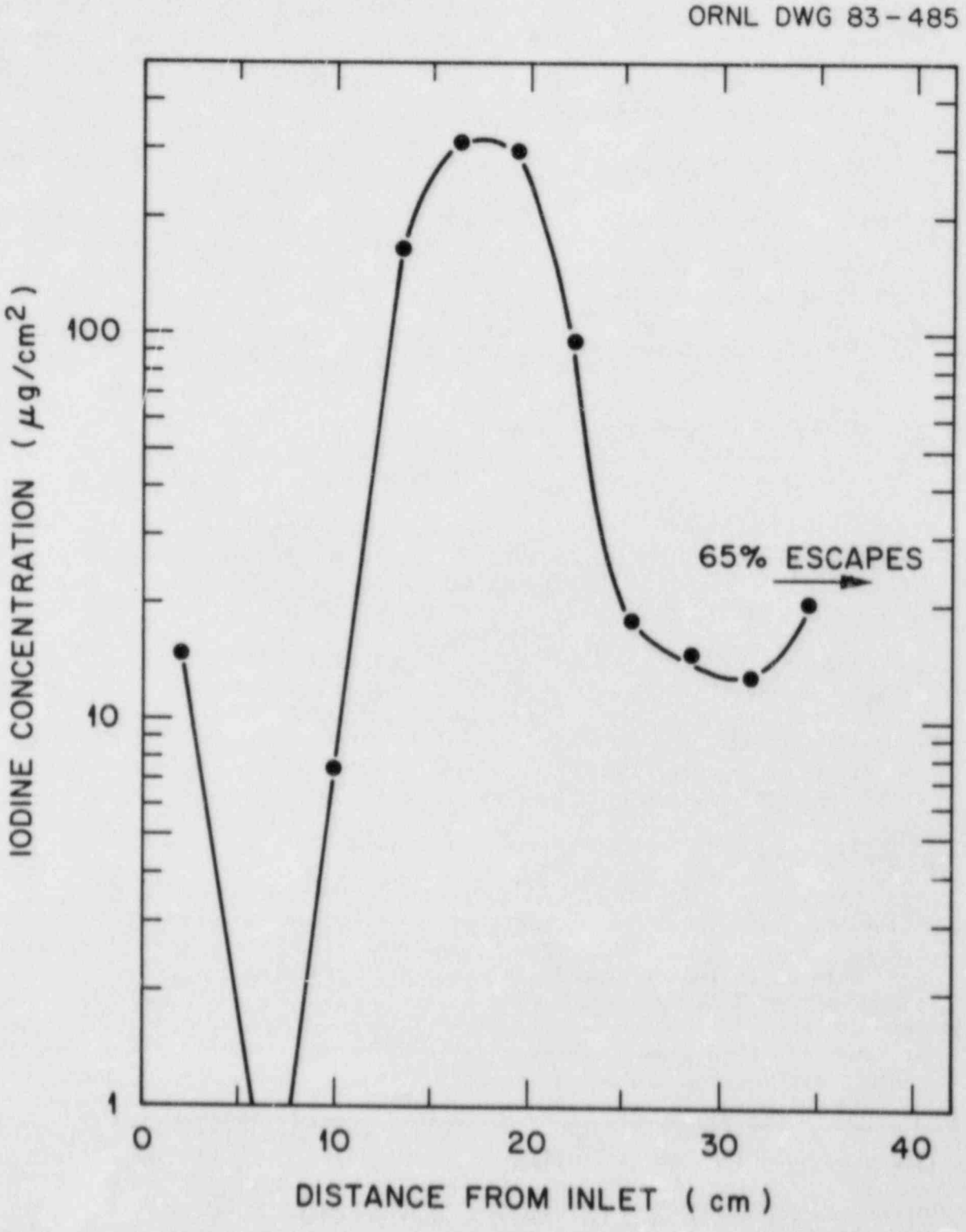

Fig. 14. Distribution of iodine in thermal gradient tube in test HI-3.

During test HI-3, 0.598 mol of gas passed down the thermal gradient tube, carrying 6.2×10^{-5} mol of iodine atoms and 6.7×10^{-4} mol of cesium atoms. If these were present as CsI and CsOH, the time-averaged partial pressures would be

CsI: 1.0×10^{-4} bar

and

CsOH: 1.0×10^{-3} bar.

Time-averaging is justified for cesium (and also for krypton) because on-line gamma spectrometry of the whole thermal gradient tube showed that ^{137}Cs accumulated at a constant rate. In the absence of time-rate data for iodine, we assume similar behavior.

The saturated vapor pressure of CsI in bar (P) over pure CsI depends on the temperature:

$$\log_{10}P = 6.243 - 9699/T \text{ (ref. 13)}, \quad (1)$$

or

$$\log_{10}P = 17.47 - 3.52 \log_{10}T - 9678/T \text{ (more modern data)}.^{14} \quad (2)$$

If pure CsI were the solid phase, we would expect no iodine to deposit above the temperature range 870 to 950 K (11 to 15 cm from the inlet to the thermal gradient tube). Since iodine was present along the entire thermal gradient, another factor must be involved.

The saturated vapor pressure of a species in solution in another is reduced as described by Raoult's law. By assuming that the solid phase on the thermal gradient tube was an ideal solid solution of CsI in CsX (an unknown species), the saturated vapor pressure over each portion can be calculated. For example, using data from Table 11 for the 6-cm (4- to 8-cm) location,

T = 1023 K at thermocouple = 1038 K at platinum.

From Eq. (2), the saturated vapor pressure of CsI over pure liquid CsI is 3.4×10^{-3} bar. As shown in Table 11, the surface concentrations of cesium and iodine were 30 and 0.22 $\mu g/cm^2$, respectively. Thus, the approximate mol fraction of iodine present (presumably as CsI) was $0.22/30 = 7.3 \times 10^{-3}$, assuming that X is monovalent. By Raoult's law, the saturated vapor pressure of CsI = $3.4 \times 10^{-3} \times 7.3 \times 10^{-3} = 2.5 \times 10^{-5}$ bar. Since the vapor pressure in the gas was greater than the saturated vapor pressure, CsI could condense, which was true at all points of the thermal gradient tube.

The iodine profile follows the cesium profile very closely. The peak represents an equilibrium between deposition and desorption of CsI molecules; as the temperature dropped, the desorption process slowed and the peaks became larger. Below 830 K, the iodine and cesium peaks decreased as molecular species were removed from the gas phase. A small part of this removal process was deposition onto the platinum surface. The major part was apparently condensation to an aerosol, because 62% of the cesium and

65% of the iodine escaped and were collected on the filter; if they had escaped as vapor, the cesium and iodine peaks in the thermal gradient tube would not have had sharp downstream cutoffs.

The iodine profile peaks where CsI is expected to condense to an aerosol throughout the gas. At the peak of the iodine profile, the average gasborne concentrations were

for I: $(65 + 35/2)\%$ of $1.0 \times 10^{-4} = 8.5 \times 10^{-3}$ bar ,

and

for Cs: $(62 + 38/2)\%$ of $1.0 \times 10^{-3} = 8.3 \times 10^{-4}$ bar .

The saturated vapor pressure over particles with this Cs/I ratio can be calculated by Raoult's law; particles may condense when the gas temperature falls below 960 K. The temperature of gas at the center of the thermal gradient tube drops below 960 K at a location 14 cm down the tube, which is where the iodine peak begins to flatten.

To summarize, iodine behavior was consistent with its release as CsI, which condensed in the thermal gradient tube to form solid deposits on the platinum and also to an aerosol, which was collected by the filters downstream. Cesium iodide condensed as a solid solution in an unidentified cesium compound, CsX.

The unidentified cesium compound does not appear to be pure CsOH, which would begin to deposit between 800 and 850 K, at 16 to 18 cm from the gas inlet of the thermal gradient tube.[15,16] The CsX must contain components less volatile than CsOH. One candidate might be Cs_2CO_3, which has a dissociation pressure of 0.125 bar at 1470 K and an enthalpy of dissociation of ~200 kJ/mol.[17,18] Cesium carbonate would deposit at all temperatures achieved in the thermal gradient tube. Another component of the mixture might be Cs_2SO_4, Cs_2SO_3, or Cs_2S. The SSMS analyses showed that considerable amounts of sulfur were present in tests HI-1, HI-2, and HI-3; a sulfurous smell has been noticed in control tests. The SSMS results reveal no other obvious candidate materials in HI-3. Carbon for the Cs_2CO_3 could come from the graphite susceptor, while sulfur could come from the furnace tube components.

3.2.5.2 Leaching of ^{137}Cs from Thermal Gradient Tubes in Tests HI-1, HI-2, and HI-3

Cesium appeared to exist in two forms: one that is soluble in the basic leach solution, and a minority constituent that is insoluble in the basic leach. They did not differ in their response to the acid leach.

The less soluble form was found on the higher-temperature parts of the thermal gradient tube. Perhaps it was intrinsically less volatile and, therefore, deposited early; it is also possible that the high temperatures may have caused a further reaction after deposition to form a less soluble compound. Some observed results are summarized as follows:

Test	Percent insoluble form below transition temperature	Transition temperature (°C)	Percent insoluble form above transition temperature
HI-1	0.5 → 2.5	~350	6 → 30
HI-2	0.14 → 0.30	~570	1.7 → 9.0
HI-3	0.3 → 2.8	~460	7 → 70

The transition temperature varied, which indicates the presence of a less volatile species whose deposition temperature varies with gas-phase concentration.

The SSMS data from test HI-2 showed that the molybdenum concentration decreased by a factor of 14 between sections 1 and 4 of the thermal gradient tube. The molybdenum/cesium atom ratio was ~6.5 on section 1 and ~0.13 on section 4. Molybdenum was the only detected element to show this effect, but unfortunately it was not found in test HI-3. Previously, SSMS data from test HI-1 showed a decrease in molybdenum/cesium ratio from 6 on sections 5 and 6 to 0.8 on sections 8 and 9; tungsten, bromine, and iodine showed a similar trend. The results of these studies are plotted in Figs. 15-17. The decontamination factor, DF, is defined as the ratio

$$\frac{^{137}\text{Cs before leaching}}{^{137}\text{Cs after leaching}} .$$

These figures illustrate the broad range of the susceptibility of the cesium forms to the basic leach, compared with the relatively constant susceptibility to the acid leach. Although the current results are insufficient to identify the chemical form of cesium involved, we will attempt to obtain positive identification through the use of other techniques.

3.2.6 Gamma Spectrometric Analysis of Fuel Specimen

The fuel specimen was counted both before and after the test in order to obtain direct counting data for comparison with the fission product inventory data generated by ORIGEN and to compare measured release values with retained-in-the-fuel values. Because of the high radioactivity level of the fuel, both distance (~10 m) and either lead attenuation (1.5 or 2.5 in.) or fractional fuel viewing (1 cm) were used to limit the gamma exposure to the detector. Several long-lived fission products were measured (as summarized in Table 12), and the values were corrected for attenuation by air, lead, and container material, if necessary, as functions of gamma-ray energy. The posttest distribution of several fission products is shown in Fig. 18. A change in fuel geometry (probably during furnace disassembly after the test) resulted in a partial void at the 7-cm position (as noted) and in corresponding minima in the fission product distribution curves. The results of quantitative analyses of these data, however, were disappointing. The measured pretest inventories were significantly lower than the corresponding ORIGEN values, ranging from ~30% of ORIGEN for ^{154}Eu to ~90% of ORIGEN for ^{137}Cs (see Table 12). Posttest

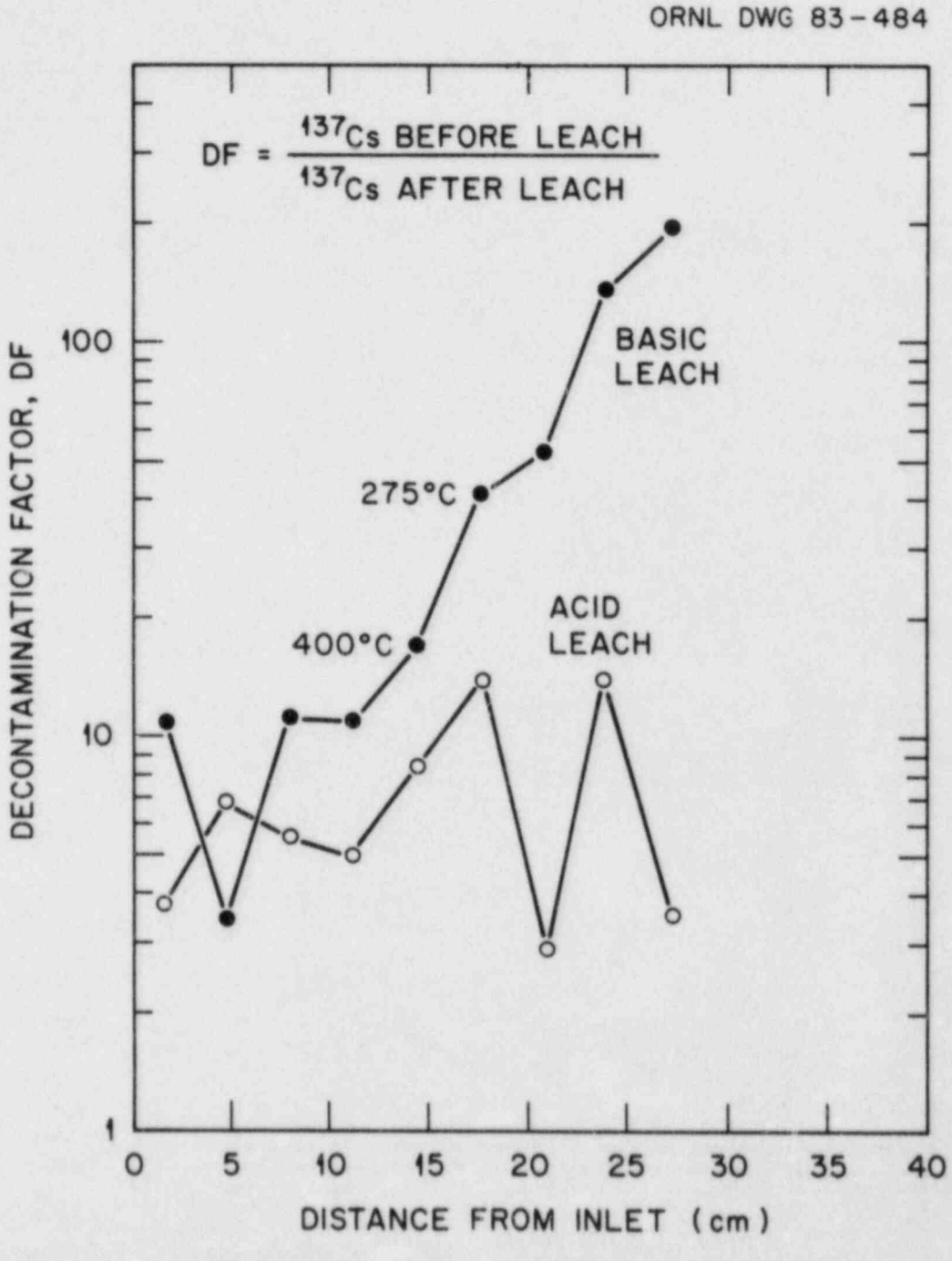

Fig. 15. Solubility of cesium deposited in thermal gradient tube of test HI-1; comparison of basic and acidic leaches.

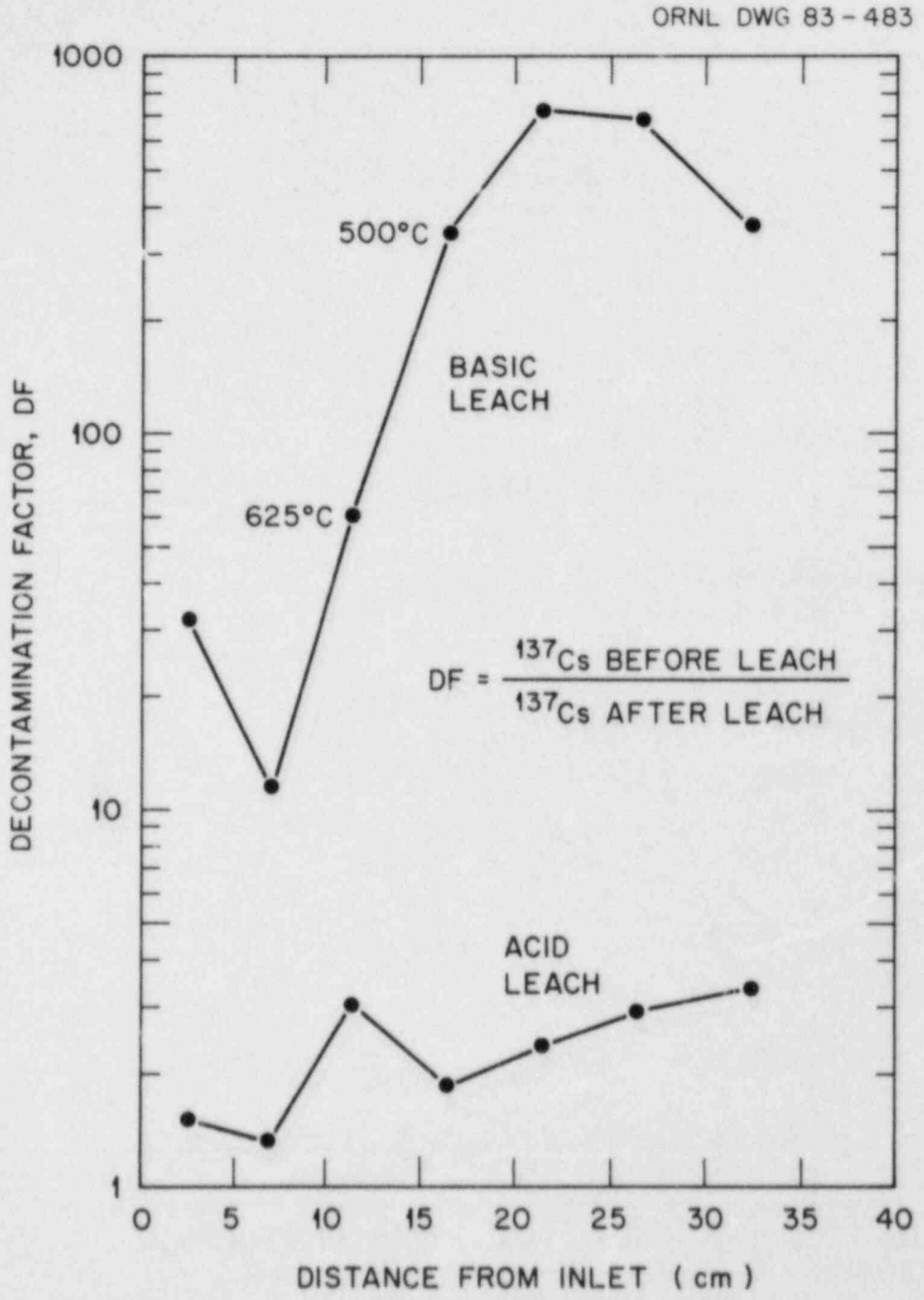

Fig. 16. Solubility of cesium deposited in thermal gradient tube of test HI-2; comparison of basic and acidic leaches.

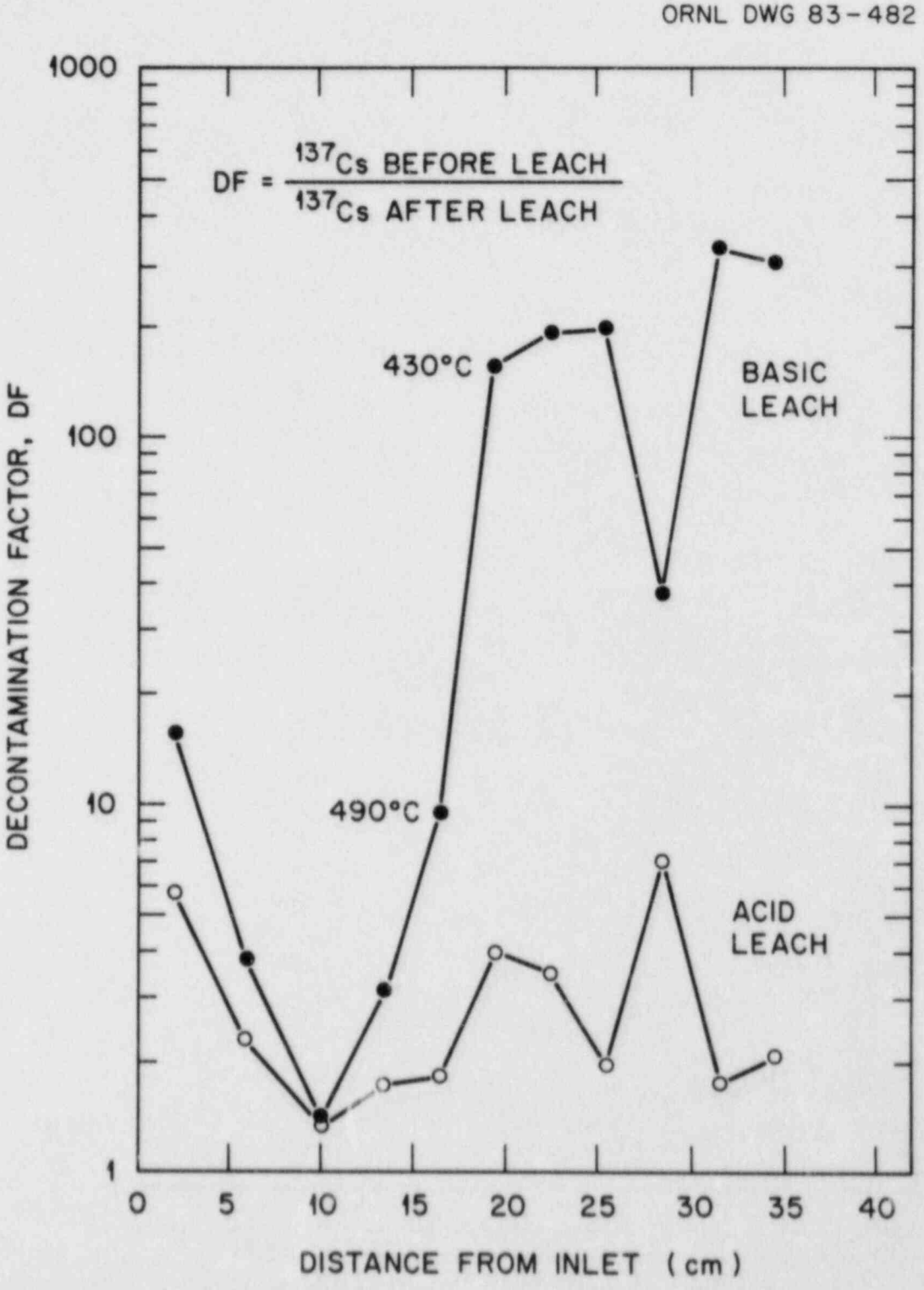

Fig. 17. Solubility of cesium deposited in thermal gradient tube of test HI-3; comparison of basic and acidic leaches.

Table 12. Comparison of fuel specimen inventory data: gamma spectrometry vs ORIGEN

Nuclide	E_γ (keV)	ORIGEN[a]	Pretest inventory (Ci)		Posttest inventory (Ci)		
			Gamma spectrometry[b]		Gamma spectrometry[b]		Scan[c]
			(1.5 in. Pb)	(2.5 in. Pb)	(1.5 in. Pb)	(2.5 in. Pb)	
^{106}Ru	1051	0.390		0.192	0.196	0.286	0.334
^{134}Cs	605	1.172	0.697	0.633	0.337	0.351	
	1365	1.172	0.784	0.827	0.340	0.324	
^{137}Cs	662	8.098	7.99	6.17	3.27	3.07	4.03
^{154}Eu	873	0.532	0.173	0.175	0.240	0.254	
	1275	0.532	0.231	0.196	0.252	0.219	0.288

[a]From Table 3, this report.

[b]The entire fuel specimen was analyzed through either a 1.5- or a 2.5-in. thickness of lead.

[c]Using a lead collimator with a 1-cm-wide viewing window, the fuel specimen was analyzed unshielded at 1-cm intervals and the measurements were summed.

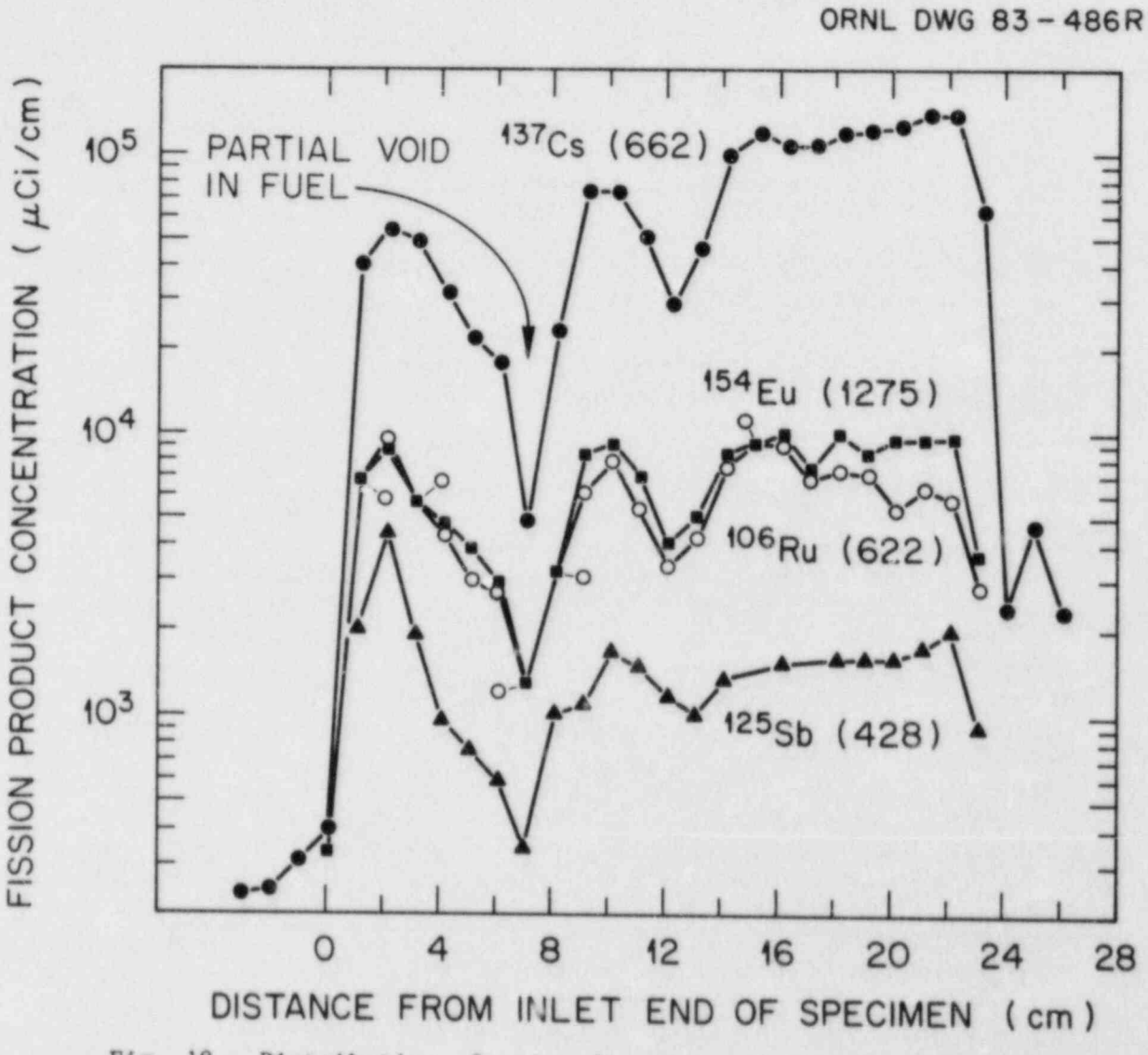

Fig. 18. Distribution of major fission products along the fuel specimen after test HI-3.

measurements added to the confusion; although large releases of cesium were indicated, the measured values for europium were higher than the pre-test values.

Tentative explanations for the low-measured inventories are as follows:

1. The gamma system was operating at ~10% below normal efficiency because of a change in cable length without readjusting the amplifier.

2. Previous gamma measurements of small H. B. Robinson fuel particles showed that ORIGEN overcalculates ^{154}Eu by almost a factor of 2.[3]

3. The higher ^{154}Eu activity measured after the test may have resulted from decreased self-shielding by the dispersed fuel.

4. The calculated corrections for gamma-ray attenuation in the UO_2, container materials, lead shielding, and air contained significant errors.

Examination of the ratios of fission products, especially for similar gamma-ray energies, yielded useful information. Variations in the ratios of different gamma rays from the same element indicate some problems with correction for attenuation, as deduced above. Ratios for ^{154}Eu (1275 keV vs 873 keV) and for ^{134}Cs (1365 keV) vs ^{154}Eu (1275 keV) are plotted in Fig. 19. The former illustrates the scatter resulting from errors in attenuation corrections. Ideally, this curve should be horizontal at 1.0; although the attenuation corrections were energy dependent, the average value (~1.14) indicates that relatively more correction (~14%) should have been made for the lower energy values. Comparison of the high-energy gamma-ray data from ^{134}Cs and ^{154}Eu should have been more accurate because the higher, more similar energies should have been affected less by attenuation errors. The approximately linear increase in this ratio shows that, compared with the relatively involatile europium, more of the volatile cesium was released from the fuel specimen at the inlet end, probably because the inlet end operated at a higher temperature. Ratios of ^{125}Sb to ^{154}Eu suggested some concentration of antimony by the unoxidized end caps, but the data were not precise enough to be conclusive.

In spite of the disagreement obtained from these measurements, we think the idea for direct measurement of retained fission products is potentially valuable and merits further effort in future tests. Unless proven otherwise, however, we will continue to use the ORIGEN data to report fractional release. More accurate determination of the attenuation factors affecting our measurements appears to be needed. Self-shielding in the fuel specimen and the effect of changes in geometry with fuel/cladding disintegration are two of the major uncertainties.

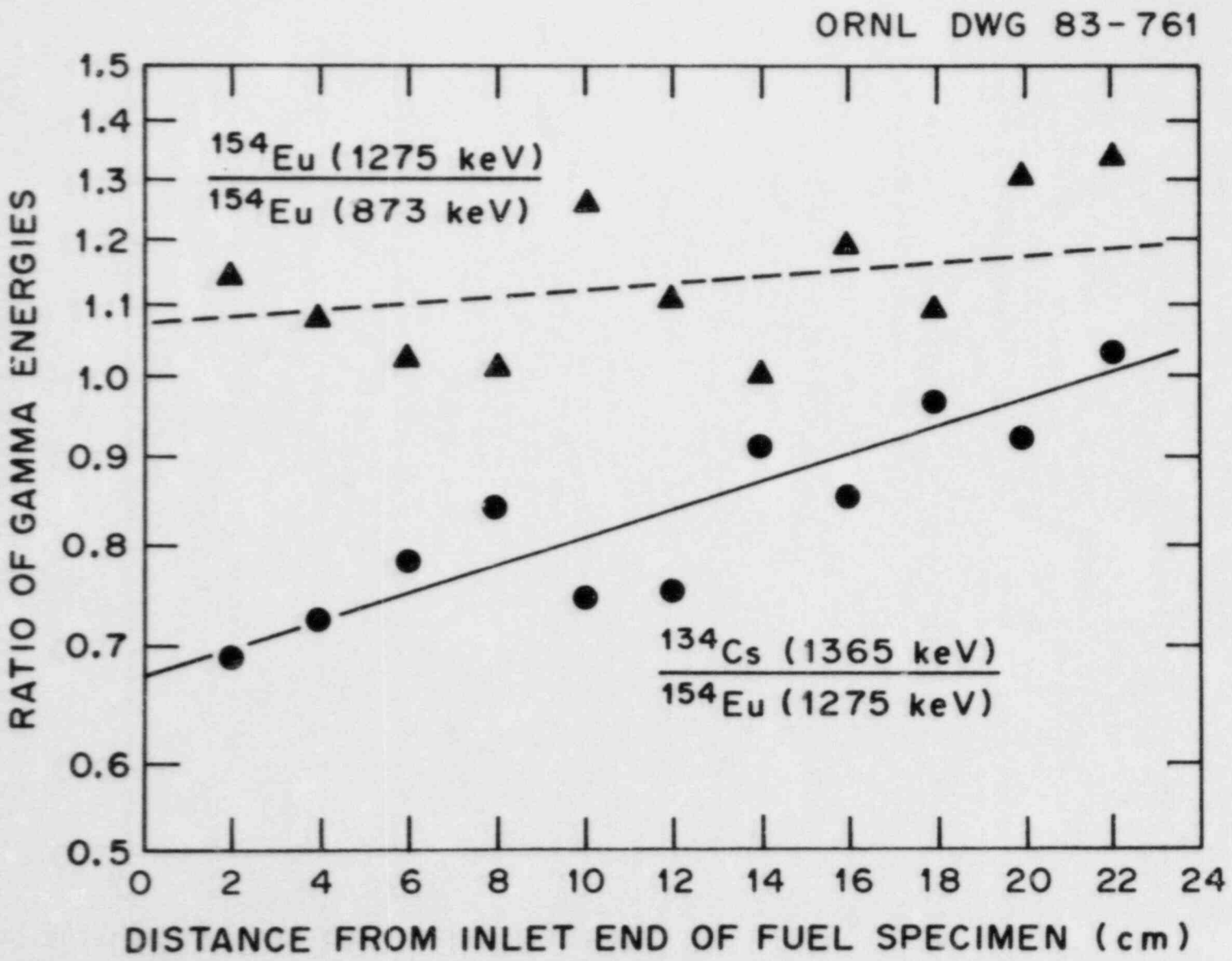

Fig. 19. Fission product distributions in test HI-3 fuel specimen, as indicated by ratios of major gamma rays.

3.2.7 Fuel Examination and Metallography

The assembly of fuel specimen and the associated ZrO_2 boats, outlet end plug, and furnace tube, all of which were encased in epoxy resin after the release test, was cut into 1-in.-long sections for inspection of the radial cross sections. These sections, which are shown in Fig. 20, illustrate the complete disintegration of the fuel specimen except for the steam inlet end (cut 1). This first section, which is ~0.2 cm from the end of the fuel rod, shows a circular section of the fuel pellet. The Zircaloy cladding and end cap surrounding it were distorted but protected from complete melting by rapid oxidation. Cuts 2 and 3 (at ~2.7 and ~5.3 cm from the end) show progressive dissolution of the UO_2 by the molten Zircaloy. Beyond cut 3, no intact UO_2 is apparent. Fusion of the Zircaloy cladding with the ZrO_2 boat is evident in cuts 3, 5, 6, and 7. It appears that significant disturbance of the fuel/cladding debris occurred during the minimal handling and injection of resin. When the assembly was inclined at an ~30° angle in order to fill it with resin, the combination of gravity and the flowing resin probably displaced pieces of debris toward the outlet end of the furnace tube.

Detailed examination and interpretation of the microstructures have not been completed; only the preliminary findings will be discussed in this report. Three of the previously discussed sections (cuts 1, 3, and 6) were prepared for metallographic examination. Sections 1 and 6 are compared in Figs. 21 and 22. All views showed extensive melting and oxidation of the Zircaloy cladding. The molten Zircaloy appeared to wet the UO_2 pellet in section 1 (Fig. 21), indicating a high oxygen content as observed by Hofmann et al.[11] In contrast, no intact fuel is apparent in section 6 (Fig. 22). Details of the oxidized cladding from section 1 are shown in Figs. 23 and 24. The bright phase penetrating the oxidized Zircaloy is probably metallic zirconium. The structures shown in Figs. 25 and 26 (from cut 6) are typical of the areas examined.

Unidentified phases were present in all three specimens; some of these exhibited appearances similar to those reported by Cook[19] and by Hofmann et al.[11] These phases are presumed to be the result of reduction and dissolution of UO_2 by molten zirconium, which forms metallic uranium and U-Zr alloys and also U-Zr-O mixtures, depending on the oxidizing conditions. Although the fuel specimen was firmly attached to the ZrO_2 boat, very little penetration of the ZrO_2 grain boundaries by the molten material was apparent (Fig. 25). Consequently, the ZrO_2 furnace tube served as a good container for the melt under these conditions. Positive identification of the reaction phases and detailed interpretation of the microstructures will be carried out during examination of these specimens at Argonne National Laboratory.

3.2.8 Activity on HI-3 Cladding Specimens after Test

Two samples of cladding were retrieved from the posttest examinations and rinsed with water to remove loosely adhering fuel. A small fraction of one sample (sample 1) was counted before analysis by SSMS.

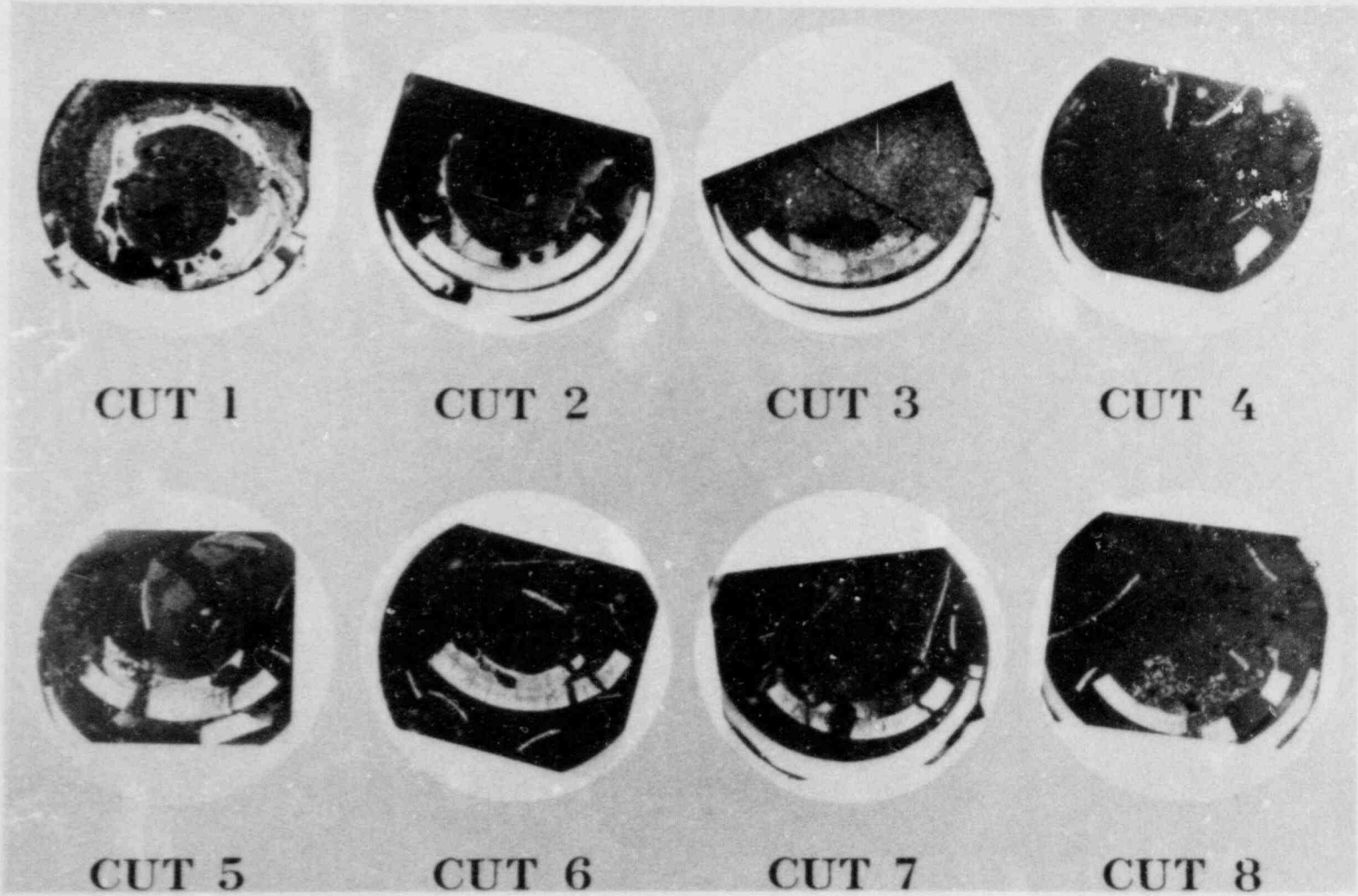

Fig. 20. Sections of the fuel specimen and ZrO_2 ceramics from test HI-3. Sections were cut at 1-in. intervals, with cut 1 at the inlet end.

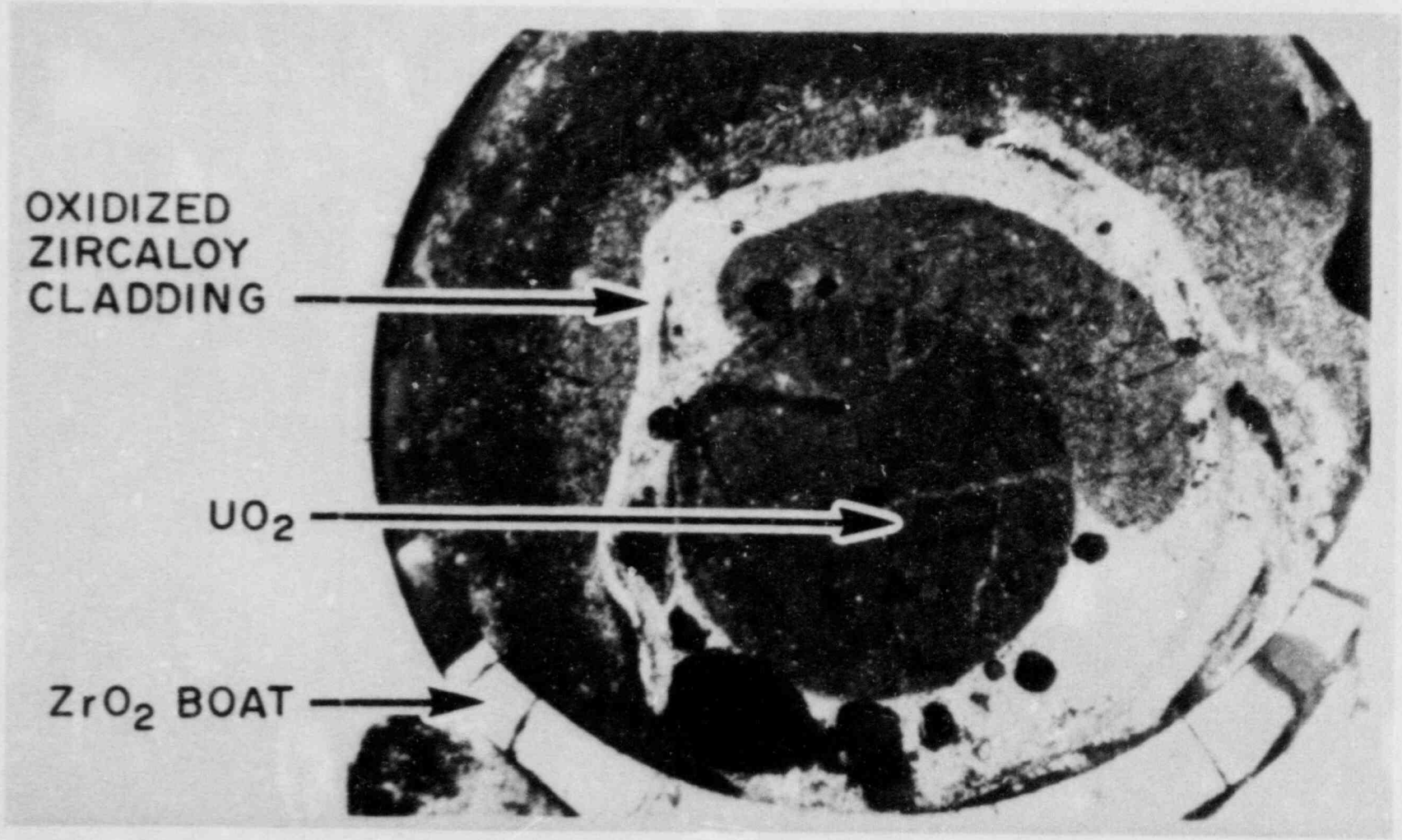

Fig. 21. Section 1 (unpolished) from test HI-3 fuel specimen. Note the full circular section of UO_2 and the oxidized, partially melted Zircaloy surrounding it (shown in greater detail in Figs. 23 and 24).

ORNL-PHOTO 4404-83

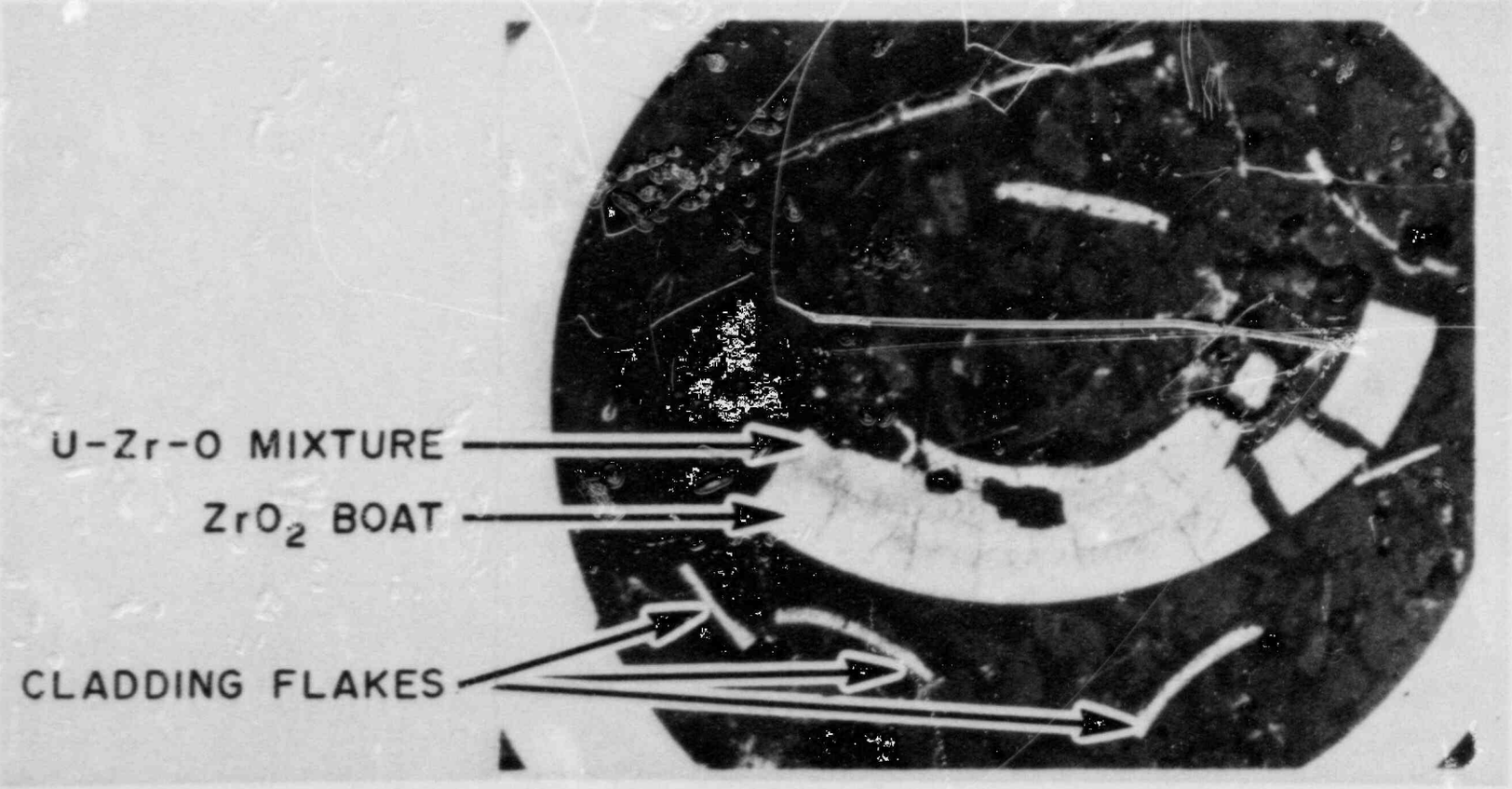

Fig. 22. Section 6 (unpolished) from test HI-3 fuel specimen. Note the fusion of the molten U-Zr-O mixture with the ZrO_2 boat, the absence of any UO_2, and several thin pieces of ZrO_2 that had formed on the outside surface of the cladding before melting.

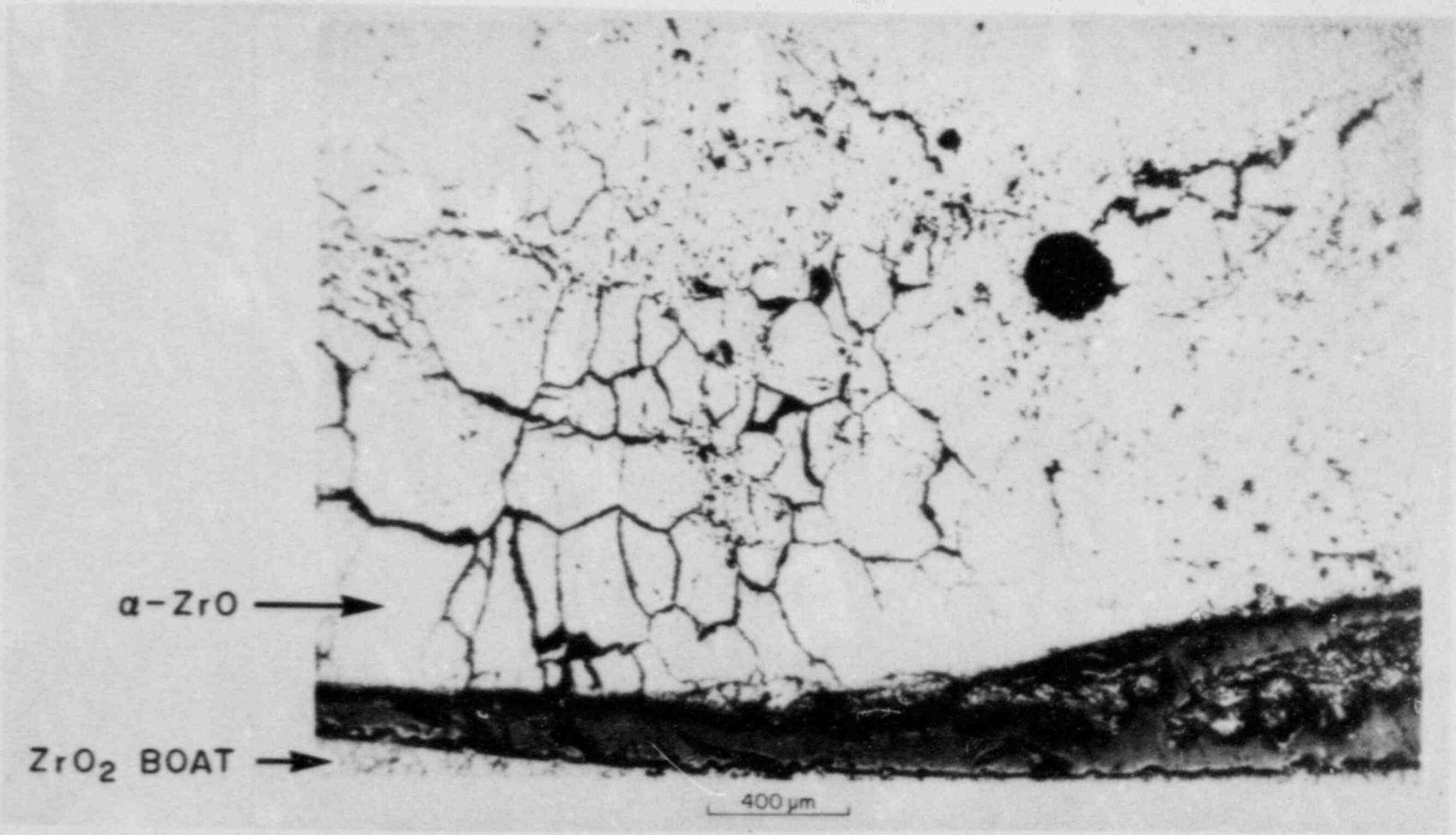

Fig. 23. Melted Zircaloy cladding material from section 1 of test HI-3 fuel specimen. Note lack of adherence to ZrO_2 boat and bright inclusions in the previously molten area.

ORNL-PHOTO 4406-83

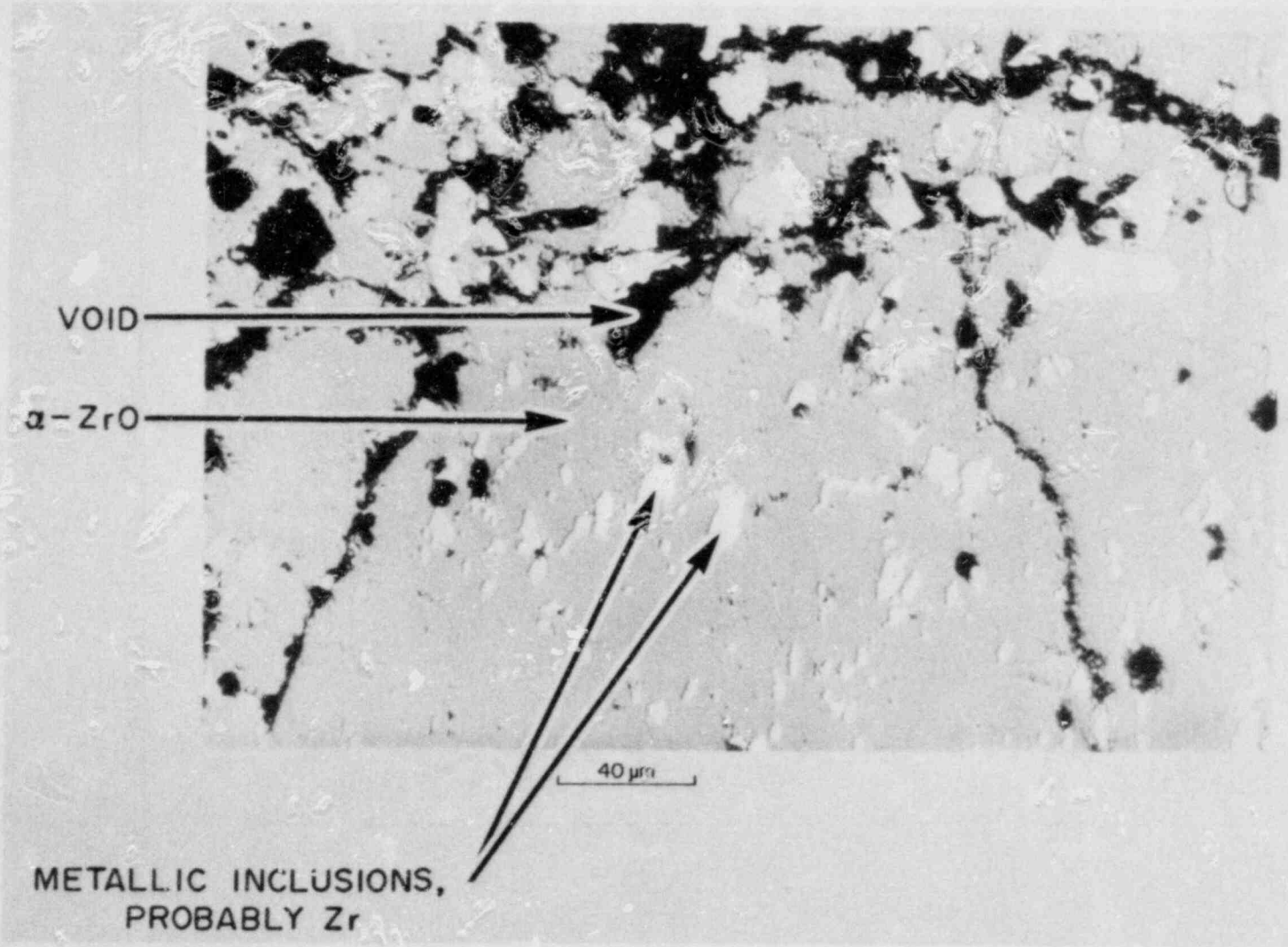

Fig. 24. Higher-magnification view of area near void in Fig. 23, showing details of inclusions and fractures.

ORNL-PHOTO 3657-83

Fig. 25. View of midlength region (cut 6) of fuel specimen from test HI-3, showing extensive melting and interaction of Zircaloy cladding and UO_2 fuel. With the exception of small chips, no intact UO_2 was found in this region.

ORNL-PHOTO 4408-83

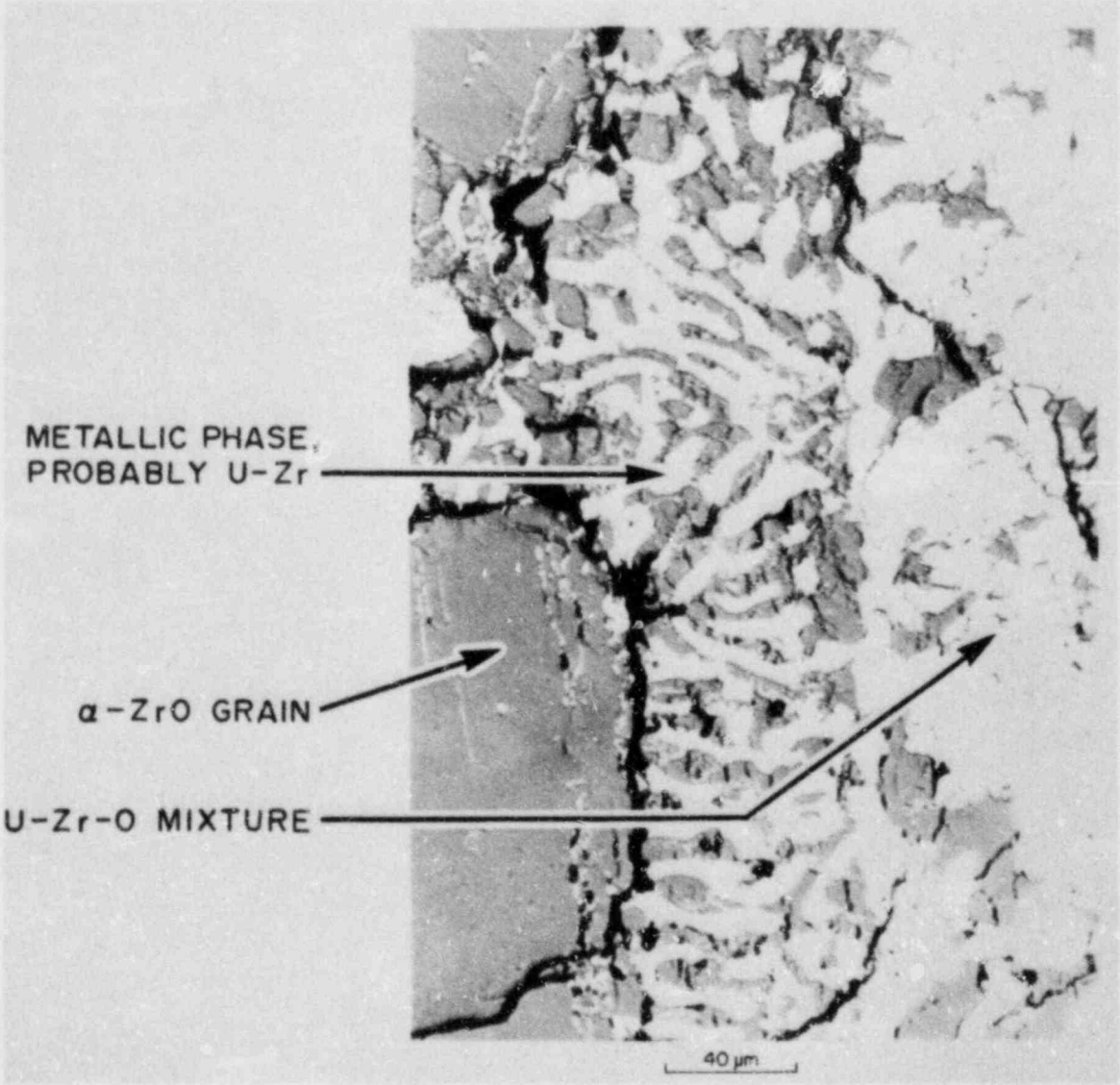

Fig. 26. Higher-magnification view of area from center of Fig. 25. Note transition from α-ZrO grain (at left) to unidentified phases, which are probably U-Zr-O mixtures (at right).

The entire second sample (sample 2) was counted. The analyses are reported in Table 13. Cerium-144 and ^{154}Eu were present with similar fractional inventories. We believe that when the fractions agree they act as tracers for fuel; thus, ~0.0045 and 0.18% of the fuel were associated with samples 1 and 2, respectively.

Table 13. Radionuclides on two samples of HI-3 cladding

Isotope	Sample 1		Sample 2	
	(μCi)[a]	(% of inventory, $\times 10^{-4}$)	(μCi)	(% of inventory, $\times 10^{-4}$)
^{60}Co	0.03		2.8	
^{106}Ru	1.4	3.6[b]	700	18.0
^{125}Sb	0.53	2.2	49	2.1
^{134}Cs	0.31	0.26	730	6.2
^{137}Cs	8.2	1.0	5300	6.5
^{144}Ce	8.2	46.0	360	20.0
^{154}Eu	23	43.0	820	15.0
$^{137}Cs/^{134}Cs$[c]	27		7.21	

[a] Activities in microcuries as of July 15, 1981.

[b] For example, read as 0.00036%.

[c] Theoretical value from ORIGEN run = 7.15; average from other HI-3 counts = 7.3.

In the HI-1, HI-2, and HI-3 series, there was progressively less ^{60}Co in the cladding as the experiment temperature rose. This conclusion is tentative because the mass of the cladding specimen in each case was unknown; the ^{60}Co content decreases relative to the ^{144}Ce content.

Ruthenium-106 followed fuel without depletion or enrichment. We reached this conclusion from the analysis of sample 2, which we judged to be more reliable because the sample was larger. Ruthenium-106 was enriched on the cladding in tests HI-1 and HI-2, presumably because it volatilized from the fuel by oxidation and decomposed by reduction on the

cladding. This did not happen in test HI-3, possibly because the molten cladding and/or the reduced steam flow rate prevented oxidation of fission products in the fuel.

Antimony-125, which was depleted in the cladding, was also absent from the rest of the fission product detection train. If samples 1 and 2 were typical of all the cladding, we must assume that either ^{125}Sb remained with the fuel (which is unlikely) or it deposited in a difficult-to-analyze part of the apparatus (e.g., the ZrO_2 ceramics).

Cesium was depleted in the cladding because it evaporated from the hot fuel rod and deposited in cooler parts of the apparatus. This conclusion is evident from analyses of samples 1 and 2. The analysis of sample 1 showed a very high $^{137}Cs/^{134}Cs$ ratio that cannot be explained.

The cesium behavior in test HI-3 differed from that in HI-1 and HI-2, where the cladding was enriched in cesium. In these tests, the cladding samples were taken from the ends of the fuel and may have been cooler, thereby allowing cesium compounds to condense.

4. SUMMARY AND CONCLUSIONS

Complete evaluation and interpretation of the results obtained in HI-3 are not within the scope of this report; the immediate objective is thorough documentation of data and observations as soon as possible after the test. Further interpretation and correlation of the data with related experiments will be included in a topical report, which will consider the results of several tests over a range of conditions. Current conclusions, therefore, are limited to the following observations:

1. Posttest data indicate that the planned test conditions — 2000°C for 20 min (see Fig. 7) with a steam flow rate of ~0.3 L/min (STP) — were accomplished with reasonable accuracy. The actual average steam flow rate was 0.36 L/min (STP).

2. The release rate data for ^{85}Kr and ^{137}Cs collected during the test (Fig. 8) are consistent with previous tests in this series. The cumulative release increased rapidly during the 2000°C phase, with a decreasing rate during the latter half of this 20-min period.

3. Based on gamma-ray spectrometry, 59.0% of the ^{85}Kr and 58.8% of the ^{137}Cs were released from the specimen during the test. In addition, small fractions of the ^{125}Sb (0.001%) and ^{110m}Ag (0.015%) were measured on components of the furnace; the high ^{137}Cs levels probably prevented measurement of similar small amounts of ^{125}Sb and ^{110m}Ag, and possibly other fission product nuclides such as ^{106}Ru, ^{144}Ce, and ^{154}Eu, on other apparatus components. The results of activation analysis for ^{129}I showed a fractional release of 35.4%, which is significantly less than the values for krypton and cesium. Unless appreciable amounts of iodine existed on a few unsampled components of the furnace (which is being investigated), no explanation for this

disagreement is apparent. Previous experiments had indicated similar fractional release rates for krypton, cesium, and iodine, as shown in Fig. 27.

4. The results of SSMS analyses were in general agreement with gamma spectrometric data. Nonradioactive fission products such as rubidium and bromine appeared to behave in the same manner as their chemical analogs, cesium and iodine. As shown by gamma spectrometry, very little silver (and tellurium, which probably behaves similarly) was found in the thermal gradient tube.

5. The cesium profile in the thermal gradient tube (Fig. 13) showed only one peak, as opposed to the more complex profile in test HI-2. The cesium distribution was essentially coincident with the iodine distribution also. The reason for this varying behavior of cesium in the thermal gradient tube (compared with that observed in previous experiments) is not understood, but varying concentrations of impurities in the systems are suspected to play a significant role and will be investigated further.

6. Both the very small amounts of ^{125}Sb and ^{110m}Ag detected and their absence from the thermal gradient tube were surprising. Since ~0.02% of the specimen inventory of ^{125}Sb was found in a very small chip of the cladding, we suspect that large fractions of the antimony and silver, and probably tellurium also, were released from the fuel but were retained in the unoxidized Zircaloy cladding. Posttest scan data for the fuel specimen showed that a large fraction of the ^{125}Sb remained in the ZrO_2 tube/fuel specimen assembly (Fig. 18).

7. The masses of aerosol collected on the thermal gradient tube (80 mg) and the filters (220 mg) appear to be consistent with test conditions and previous experiments.

8. The fuel specimen was inspected only through a series of radial cross sections because the cladding melted and fused to the ZrO_2 boat and furnace tube. These cross sections showed that the fuel remained intact only at the inlet end where the cladding was oxidized by the incoming steam before melting. Most of the specimen had disintegrated into rubble as a result of UO_2 dissolution by molten Zircaloy, with posttest handling probably being a contributing factor.

9. Three of the radial sections were examined metallographically. Observation of these specimens included wetting of the UO_2 by molten Zircaloy, oxidation of the Zircaloy to form areas of α-Zr(O) and ZrO_2, and the formation of several unidentified phases that probably resulted from Zr-UO_2 interactions. Additional studies using specialized techniques (e.g., scanning electron micrography and microprobe analysis) should provide phase identification and clarify the reactions that occurred in these areas.

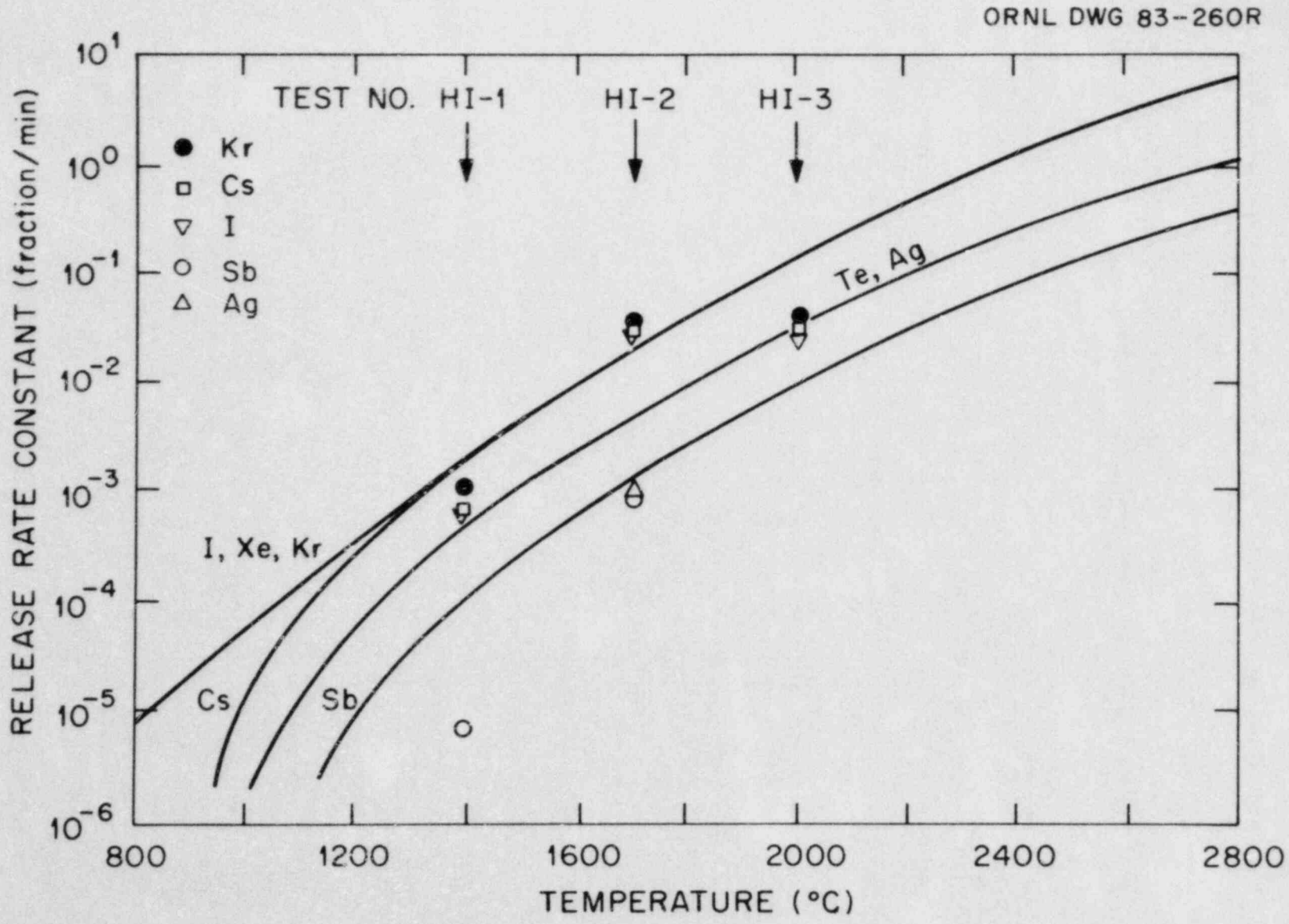

Fig. 27. Release rate data for tests HI-1, HI-2, and HI-3, compared with curves from NUREG-0772.

5. REFERENCES

1. M. F. Osborne, R. A. Lorenz, and R. P. Wichner, "Program Plan for Fission Product Release from LWR Fuel in Steam," memorandum to USNRC, April 1982.

2. R. A. Lorenz, J. L. Collins, A. P. Malinauskas, O. L. Kirkland, and R. L. Towns, Fission Product Release from Highly Irradiated LWR Fuel, NUREG/CR-0722 (ORNL/NUREG/TM-287/R2), February 1980.

3. R. A. Lorenz, J. L. Collins, A. P. Malinauskas, M. F. Osborne, and R. L. Towns, Fission Product Release from Highly Irradiated LWR Fuel Heated to 1300-1600°C in Steam, NUREG/CR-1386 (ORNL/NUREG/TM-346), November 1980.

4. R. A. Lorenz, J. L. Collins, M. F. Osborne, R. L. Towns, and A. P. Malinauskas, Fission Product Release from BWR Fuel Under LOCA Conditions, NUREG/CR-1773 (ORNL/NUREG/TM-388), July 1981.

5. R. A. Lorenz, J. L. Collins, and A. P. Malinauskas, Fission Product Source Terms for the LWR Loss-of-Coolant Accident, NUREG/CR-1298 (ORNL/NUREG/TM-321), July 1980.

6. M. F. Osborne, R. A. Lorenz, J. R. Travis, and C. S. Webster, Data Summary Report for Fission Product Release Test HI-1, NUREG/CR-2928 (ORNL/TM-8500), December 1982.

7. M. F. Osborne, R. A. Lorenz, J. R. Travis, C. S. Webster, and K. S. Norwood, Data Summary Report for Fission Product Release Test HI-2, NUREG/CR-3171 (ORNL/TM-8667), in press.

8. P. E. MacDonald to A. P. Malinauskas, Transmittal of CPL Assembly B05 Axial Flux Measurements, MacD-76-75, Sept. 11, 1975.

9. M. F. Osborne and G. W. Parker, The Effect of Irradiation on the Failure of Zircaloy-Clad Fuel Rods, ORNL-TM-3626, January 1972.

10. H. Albrecht, M. F. Osborne, and H. Wild, "Experimental Determination of Fission and Activation Product Release During Core Meltdown," Proceedings of Thermal Reactor Safety Meeting, Sun Valley, Idaho, Aug. 1-4, 1977.

11. P. Hofmann, D. Kerwin-Peck, and P. Nikolopolous, "Physical and Chemical Phenomena Associated with the Dissolution of Solid UO_2 by Molten Zircaloy-4," paper presented at the Sixth International Conference on Zirconium in the Nuclear Industry, Vancouver, British Columbia, Canada, June 28-July 1, 1982.

12. R. C. Weast, ed., Handbook of Chemistry and Physics, The Chemical Rubber Co., Cleveland, Ohio, 1966.

13. N. A. Lange, comp., ed., Handbook of Chemistry, 9th ed., McGraw, New York, 1956, p. 1426.

14. I. Barin and O. Knacke, Thermochemical Properties of Inorganic Substances, Springer-Verlag, Berlin, 1973, p. 254.

15. J. L. Collins, ORNL, personal communication, January 1983.

16. R. A. Sallach and R. Elrick, Sandia National Laboratory, personal communication to K. S. Norwood, Guest Scientist at ORNL, 1983.

17. J. C. Bailor et al., ed., Comprehensive Inorganic Chemistry, vol. 1, Pergamon, New York, 1973, p. 458.

18. I. Barin and O. Knacke, Thermochemical Properties of Inorganic Substances: Supplement, Springer-Verlag, Berlin, 1977, pp. 216-19.

19. B. A. Cook, Fuel Rod Material Behavior During Test PCM-1, NUREG/CR-0757, EG&G Idaho, June 1979.

20. R. B. Rird, W. E. Steward, and E. N. Lightfoot, Transport Phenomena, Wiley, New York, 1960.

21. N. A. Lange, comp., ed., Handbook of Chemistry, 9th ed., McGraw, New York, 1956, p. 1541.

22. N. A. Lange, comp., ed., Handbook of Chemistry, 9th ed., McGraw, New York, 1956, p. 1542.

Appendix A. RADIAL TEMPERATURE DISTRIBUTION IN THE THERMAL GRADIENT TUBE

Average gas flow rate = 0.596 mol in 20 min
= $0.596/20 \times 60 = 4.97 \times 10^{-4}$ mol/s;

approximate heat capacity at constant pressure = 29.5 $J \cdot K^{-1} \cdot mol^{-1}$ (ref. 20) (assuming ideality);

approximate gas inlet temperature = 1400 K (in HI-1, when fuel was at 1673 K, the gas was hot enough to melt gold at 1336 K);

approximate gas outlet temperature = 423 K (assuming the gas has been cooled to the temperature of the thermal gradient tube);

therefore, the thermal gradient tube must reject $4.97 \times 10^{-4} \times 29.5 \times (1400-423) = 14.3$ $J \cdot s^{-1}$ of heat.

The platinum liner, which is 36 cm long and 3 mm in diameter, is the heat transfer surface.

Area of heat transfer surface = $\pi dt = \pi \times 0.003 \times 0.36 = 3.39 \times 10^{-3}$ m^2;

average heat flux = $14.3/3.39 \times 10^{-3} = 4.22 \times 10^3$ $W \cdot m^{-2}$.

Gas thermal conductivities increase with temperature. A typical value for $He/H_2/H_2O$ mixtures at 900 K is calculated to be 0.218 $W \cdot K^{-1} \cdot m^{-1}$ (ref. 21); therefore, the temperature gradient in the gas adjacent to the wall is:

$$4.22 \times 10^3/0.218 = 1.94 \times 10^4 \ K \cdot m^{-1} .$$

The radial temperature profile in the gas is approximately parabolic because the flow is laminar:

$$T_r = (T_c - T_w)(1 - r^2/r_w^2) + T_w ,$$

where

T_r = temperature at radius r,
T_c = temperature at center,
T_w = temperature at wall,
r_w = position of wall,
r = arbitrary radial position.

Temperature gradient at the wall = $-2(T_c - T_w)/r_w$;

temperature drop across the bulk gas = $1.94 \times 10^4/2 \times 1.5 \times 10^{-3} = 14.6$ K;

thermal conductivity of platinum = 69.9 $W \cdot K^{-1} \cdot m^{-1}$ (ref. 22).

The thermal gradient across the platinum is $4.22 \times 10^3/69.9 = 60.4\ K \cdot m^{-1}$; since the platinum is 10^{-4} m thick, the temperature drop across it is

$$60.4 \times 10^{-4} = 0.006\ K.$$

Possible thickness of gas gap between the platinum and the quartz = 10^{-4} m;

temperature drop across gap = $1.94 \times 10^4 \times 10^{-4} = 1.9$ K;

thermal conductivity of quartz = 1.91 $W \cdot K^{-1} \cdot m^{-1}$ (ref. 22);

temperature gradient across quartz = $4.22 \times 10^3/1.19 = 2.21 \times 10^3\ K \cdot m^{-1}$.

Since the quartz is 2×10^{-3} m thick, the temperature drop is

$$2.21 \times 10^3 \times 2 \times 10^{-3} = 4.4\ K.$$

To summarize, typical temperatures relative to the temperature on the outside wall of the quartz thermal gradient tube were:

thermocouple	= x K,
inside surface of the platinum	= x +6 K, and
center gas temperature	= x +21 K.

NUREG/CR-3335
ORNL/TM-8793
Dist. Category R3

INTERNAL DISTRIBUTION

1. R. E. Adams
2. C. W. Alexander
3. E. C. Beahm
4. J. T. Bell
5. D. O. Campbell
6. J. L. Collins
7. R. W. Glass
8. J. H. Goode
9. J. R. Hightower
10. T. S. Kress
11. C. E. Lamb
12. R. E. Leuze
13-17. R. A. Lorenz
18. A. P. Malinauskas
19. K. S. Norwood
20-24. M. F. Osborne
25. W. W. Pitt
26. J. H. Shaffer
27. R. D. Spence
28. M. G. Stewart
29. O. K. Tallent
30. R. L. Towns
31-32. J. R. Travis
33-34. C. S. Webster
35. S. K. Whatley
36. R. P. Wichner
37. R. G. Wymer
38. Central Research Library
39. ORNL-Y-12 Technical Library Document Reference Section
40. Laboratory Records
41. Laboratory Records, ORNL-RC
42. ORNL Patent Section

EXTERNAL DISTRIBUTION

43. Office of Assistant Manager for Energy Research and Development, ORO-DOE, P.O. Box E, Oak Ridge, TN 37831
44. Director, Division of Reactor Safety Research, U.S. Nuclear Regulatory Commission, Washington, DC 20555
45-46. Technical Information Center, DOE, Oak Ridge, TN 37831
47. Division of Technical Information and Document Control, U.S. Nuclear Regulatory Commission, Washington, DC 20555
48. L. K. Chan, U.S. Nuclear Regulatory Commission, Fuel Systems Research Branch, Division of Accident Evaluation, U.S. Nuclear Regulatory Commission, Washington, DC 20555
49. M. Jankowski, Fuel Research Systems Branch, Division of Accident Evaluation, U.S. Nuclear Regulatory Commission, Washington, DC 20555
50. R. V. Strain, Argonne National Laboratory, 9700 South Cass Avenue, Argonne, IL 60439
51-325. Given distribution as shown in Category R3 (NTIS – 10)

NRC FORM 335 (11.81)

U.S. NUCLEAR REGULATORY COMMISSION

BIBLIOGRAPHIC DATA SHEET

1. REPORT NUMBER (Assigned by DDC)
NUREG/CR-3335
(ORNL/TM-8793)

4. TITLE AND SUBTITLE (Add Volume No., if appropriate)

Data Summary Report for Fission Product Release Test HI-3

2. (Leave blank)

3. RECIPIENT'S ACCESSION NO.

7. AUTHOR(S)
M. F. Osborne, R. A. Lorenz, K. S. Norwood, J. R. Travis, and C. S. Webster

5. DATE REPORT COMPLETED
MONTH: August YEAR: 1983

9. PERFORMING ORGANIZATION NAME AND MAILING ADDRESS (Include Zip Code)

Oak Ridge National Laboratory
P.O. Box X
Oak Ridge, TN 37830

DATE REPORT ISSUED
MONTH: March YEAR: 1984

6. (Leave blank)

8. (Leave blank)

12. SPONSORING ORGANIZATION NAME AND MAILING ADDRESS (Include Zip Code)

Division of Accident Evaluation
Office of Nuclear Regulatory Research
U.S. Nuclear Regulatory Commission
Washington, D.C. 20555

10. PROJECT/TASK/WORK UNIT NO.

11. FIN NO.
B0127

13. TYPE OF REPORT
Data Summary

PERIOD COVERED (Inclusive dates)
August 1983 – March 1984

15. SUPPLEMENTARY NOTES

14. (Leave blank)

16. ABSTRACT (200 words or less)

The third in a series of high-temperature fission product release tests was conducted for 20 min at 2000°C in flowing steam. The test specimen, a 20-cm-long section of H. B. Robinson fuel rod that had been irradiated to ~25,200 MWd/t, was heated in an induction furnace in a hot cell.

Posttest examination showed that the Zircaloy cladding had melted, causing extensive disintegration of the UO_2 fuel and formation of molten phases that appeared to be rich in uranium. Analyses of test components revealed very high fractional releases of ^{85}Kr (59.0%), ^{137}Cs (58.8%), and ^{129}I (35.4%). The releases of ^{125}Sb and ^{110m}Ag, however, were much less than those observed in test HI-2 at 1700°C, perhaps as a result of lower steam flow rate in test HI-3. The extent of aerosol formation, as evidenced by mass of material collected on filters, was similar in the two tests.

17. KEY WORDS AND DOCUMENT ANALYSIS

17a. DESCRIPTORS

Fission product
Fission product release

17b. IDENTIFIERS/OPEN-ENDED TERMS

18. AVAILABILITY STATEMENT

19. SECURITY CLASS (This report)
Unclassified

21. NO. OF PAGES

20. SECURITY CLASS (This page)
Unclassified

22. PRICE
$